

Wavelet Analysis Based Image Fusion

*A dissertation submitted in partial fulfilment
of the requirements for the degree of
BACHELOR OF TECHNOLOGY*

IN

ELECTRONICS & COMMUNICATION ENGINEERING

Under the guidance of

DR. SUDIPTA MAJUMDAR

By

AAKRITI YADAV (2K10/EC/002)

BHUVI CHOPRA (2K10/EC/045)

DHWANI KAPOOR (2K10/EC/053)

EKTA SENGAR (2K10/EC/056)



DELHI TECHNOLOGICAL UNIVERSITY

2010-2014

CERTIFICATE

This is to certify that the dissertation “Wavelet Analysis Based Image Fusion” submitted by Aakriti Yadav (2K10/EC/002), Bhuvni Chopra (2K10/EC/045), Dhvani Kapoor (2K10/EC/053) and Ekta Sengar (2K10/EC/056) towards the partial fulfilment of the requirements for the award of Bachelor of Engineering degree in Electronics and Communication Engineering at Delhi Technological University is an authentic work carried out by them under my supervision and guidance.

It is further certified that this dissertation has not been earlier submitted in part or full to any university for any degree or diploma.

Dr. Sudipta Majumdar

Assistant Professor

Electronics and Communication Engineering

Delhi Technological University

Delhi-42

ACKNOWLEDGEMENT

We would like to express our heartfelt gratitude to Dr. Sudipta Majumdar for her constant motivation, support and guidance that helped us in completing our project in a satisfactory and fulfilling manner. The entire experience has been a great learning expedition and has exposed us to newer frontiers of technology.

We are thankful to Delhi Technological University for giving us the opportunity to undertake the project in area of our interest. Our association with the faculty and staff has been a good learning experience and has provided us with invaluable feedback.

AAKRITI YADAV (2K10/EC/002)

BHUVI CHOPRA (2K10/EC/045)

DHWANI KAPOOR (2K10/EC/053)

EKTA SENGAR (2K10/EC/056)

ABSTRACT

Everywhere around us are signals that can be analyzed. For example, there are seismic tremors, human speech, engine vibrations, medical images, financial data, music, and many other types of signals. Wavelet analysis is a new and promising set of tools and techniques for analyzing these signals and extracting information from them.

The main motivation for this project is to detect certain textures and features that may be localized by performing image fusion using wavelets and fuzzy logic and hence employ these measures to produce better image fusion algorithms. These algorithms can then be deployed for medical images, image enhancement and fault detection. Some medical domains are very productive. We can find studies on micro-potential extraction in EKGs, on time localization of His bundle electrical heart activity, in ECG noise removal. In EEGs, a quick transitory signal is drowned in the usual one. The wavelets are able to determine if a quick signal exists, and if so, can localize it. There are attempts to enhance mammograms to discriminate tumours from calcifications.

TABLE OF CONTENTS

Acknowledgement.....	2
Abstract.....	3
1. Introduction.....	9
2. Wavelet Analysis.....	12
2.1 Wavelet Families.....	12
2.2 Continuous Wavelet Transform (CWT)	14
2.3 Discrete Wavelet Transform (DWT)	16
2.4 2-D Discrete Wavelet Transform.....	17
2.5 Wavelet Reconstruction.....	18
2.6 Comparison among Fourier transform, short-time Fourier transform (STFT) and Wavelet Transform.....	19
2.7 Applications of Wavelet.....	20
2.8 Wavelet Toolbox.....	20
3. Texture Classification.....	23
3.1 Wavelet Transform of Image.....	24
3.2 Texture Training.....	24
3.3 Texture Classification.....	25
3.4 Noise Introduction.....	26
3.5 Algorithm.....	26
3.6 Result and Discussion.....	27
3.7 Future Application.....	29
4. Image Fusion.....	30
4.1 Image Fusion Methods.....	32
4.2 Wavelet Based Image Fusion.....	32
5. Fog Degraded Image Enhancement.....	34
5.1 Homomorphic Filtering.....	34
5.2 Histogram Equalization.....	36
5.3 Wavelet Fusion Method Analysis.....	37
5.4 Non Linear Gain Function.....	38
5.5 Algorithm.....	40
5.6 Result and Discussion.....	40
6. Vessel Segmentation in X-Ray Image.....	42
6.1 Vesselness Filter.....	42

6.2 Vessel Segmentation.....	44
6.3 Algorithm.....	45
6.4 Result and Discussion.....	45
7. Texture Fusion of CT/MRI Images.....	47
7.1 Texture Feature Extraction.....	47
7.2 Wavelet Based Texture Fusion.....	48
7.3 Algorithm.....	50
7.4 Comparison with other method.....	50
7.5 Result and Discussion.....	50
8. High Capacity Steganography.....	52
8.1 An overview of Internet Security.....	52
8.2 Steganography Techniques.....	53
8.3 High Capacity And Security Steganography.....	54
8.4 Still Imagery Steganography.....	55
8.5 Data Hiding Requirements.....	55
8.6 Algorithm.....	56
8.7 Analysis.....	57
8.8 Result and Discussion.....	58
Conclusion.....	62
References.....	63

LIST OF FIGURES

Fig. 2.1 Haar Wavelet.....	12
Fig. 2.2 The Daubechies family Wavelets.....	13
Fig. 2.3 Mexican Hat Wavelet.....	13
Fig. 2.4 The Biorthogonal family of Wavelets.....	13
Fig. 2.5 The Symlets family of Wavelets.....	14
Fig. 2.6 Calculation of CWT.....	15
Fig. 2.7 Shifting Operation.....	15
Fig. 2.8 Scaling Operation.....	15
Fig. 2.9 Filtering Process.....	16
Fig. 2.10 Calculation of DWT coefficients	17
Fig. 2.11(a) Calculation of approximate and detailed coefficients of 2D DWT.....	17
Fig. 2.11(b) Calculation of approximate and detailed coefficients of 2D DWT.....	18
Fig. 2.12 3 Level Wavelet Image Decomposition.....	18
Fig. 2.13 Inverse Wavelet Transform.....	19
Fig. 2.14 Comparison among Fourier Transform, Short Time Fourier Transform And Wavelet Transform.....	19
Fig. 3.1 Different textures in real world.....	23
Fig. 3.2 Texture training.....	24
Fig. 3.3 Texture Classification.....	26
Fig. 3.4 Sponge.....	28
Fig. 3.5 Sandpaper.....	28
Fig. 3.6 Orange Peel.....	28
Fig. 3.7 Linen.....	28
Fig. 3.8 Cracker.....	28
Fig. 3.9 Cotton.....	28
Fig. 3.10 Foam.....	28
Fig. 3.11 Brown Bread.....	28
Fig. 3.12 Aluminium Foil.....	28
Fig. 3.13 Test Image.....	28
Fig. 3.14 Image with Salt and Pepper noise.....	28
Fig. 3.15 Application in CT scan.....	29
Fig 3.16 Application in satellite image.....	29
Fig. 4.1 Image fusion for an IKONOS scene for Cairo, Egypt.....	30
(a) multispectral low resolution input image	
(b) panchromatic high resolution input image	
(c) fused image of IHS	
Fig. 4.2 CCD visual images with the.....	30
(a) right and	
(b) left clocks out of focus, respectively;	
(c) the resulting fused image from (a) and (b) with the two clocks in focus.	

Fig. 4.3 Images captured from the.....	31
(a) visual sensor and	
(b) infrared sensor, respectively;	
(c) the resulting fused image from (a) and (b) with all interesting details in focus.	
Fig. 4.4 (a) MRI and.....	31
(b) PET images;	
(c) fused image from (a) and (b).	
Fig. 4.5 Fusion of the wavelet transforms of two images.....	33
Fig. 5.1 Homomorphic filtering in frequency domain.....	36
Fig. 5.2 Wavelet Fusion Model.....	38
Fig. 5.3 The curve of $f(x)$ when $b = 0.25$ and $c = 25$	39
Fig. 5.4 Results of the contrastive test.....	40
Fig 6.1 Original Angiographic Image.....	46
Fig 6.2 Vesselness Filtered Image.....	46
Fig. 6.3 Fused Image.....	46
Fig. 6.4 High Threshold Image.....	46
Fig. 6.5 Low Threshold Image.....	46
Fig. 6.6 Combined Final Image.....	46
Fig. 7.1 MRI of brain.....	51
Fig. 7.2 CT scan of brain.....	51
Fig. 7.3 Fused image by the proposed method.....	51
Fig. 7.4 Fused image by other method.....	51
Fig. 7.5 MRI of abdomen.....	51
Fig. 7.6 CT of abdomen.....	51
Fig. 7.7 Fused image.....	51
Fig. 8.1 Process flow of secretly transmitting data. Using steganography, private data remains undetectable until it reaches its intended audience.....	54
Fig. 8.2 Cover image, Payload image, Stego image and Extracted image for $\alpha = 0.007$	58
Fig. 8.3 Cover image, Payload image, Stego image and Extracted image for $\alpha = 0.02$	59
Fig. 8.4 Cover image, Payload image, Stego image and Extracted image for $\alpha = 0.07$	60
Fig. 8.5 Cover image, Payload image, Stego image and Extracted image for $\alpha = 0.07$	61

LIST OF TABLES

Table 2.1 Wavelet families in the toolbox.....	22
Table 5.1 Quantitative analysis of results of Fig. 5.4.....	41
Table 6.1 Possible patterns in 2D and 3D, depending on the value of the eigenvalues λ_k (H=high, L=low, N=noisy, usually small, +/- indicate the sign of the eigenvalue). The eigenvalues are ordered: $ \lambda_1 \leq \lambda_2 \leq \lambda_3 $	44
Table 8.1 Performance comparison for different values of alpha (α).....	61

1. INTRODUCTION

The main objective of this project is to detect certain textures and features that may be localized by performing image fusion using wavelets and hence employ these measures to produce better image fusion algorithms. These algorithms are then deployed for texture classification, image enhancement, medical images, and data hiding in images.

Wavelets are short wavelike functions that can be scaled and translated. Wavelet transforms take any signal and express it in terms of scaled and translated wavelets. The resulting wavelet transform is a representation of the signal at different scales. The transform allows manipulation of features at different scales independently, such as suppressing or strengthening some particular feature. Wavelets have scale aspects and time aspects; consequently every application has scale and time aspects. As compared with other transforms such as Fourier Transform and Short Time Fourier Transform, Wavelet Transform gives better result in many applications as it uses both time and scale aspects. Due to the numerous multi-scale transforms, different fusion rules will be proposed for different purpose and applications.

One of the applications of Wavelet Transform is in texture analysis and classification in an image. Texture is a property that represents the surface and structure of an image. Image textures are complex visual patterns composed of entities or regions with sub-patterns with the characteristics of brightness, color, shape, size, etc. Texture can be regarded as a similarity grouping in an image. The dimensions of texture cannot be same; hence to represent texture with a single method is not possible. Texture analysis is a major step in texture classification, image segmentation and image shape identification tasks. Descriptors providing measures of properties such as smoothness, coarseness and regularity are used to quantify the texture content of an object. In our project, texture classification is proposed with the help of wavelet transform. Texture classification using wavelet statistical features, wavelet co-occurrence features and to combine both the features namely wavelet statistical and co-occurrence features of wavelet transformed images with different feature databases is performed and discussed.

Image fusion is the process that combines information from multiple images of the same scene. The result of image fusion is a new image that retains the most desirable information and characteristics of each input image. It has been found that the standard fusion methods perform well spatially but usually introduce spectral distortion. To overcome this problem, numerous multi-scale transform based fusion schemes will be proposed. We will focus on

fusion methods based on the discrete wavelet transform (DWT), the most popular tool for image processing.

Wavelet transform is also used in enhancement of fog-degraded image. Fog is a very common weather phenomena which produces whitening effect and causes the image to degenerate and become fuzzy. Therefore, it has very vital practical significance for strengthening the contrast gradient and the image detail information from the fog-degraded image. Wavelet transform, histogram equalization and non-linear operator are used to process synthetically fog-degraded Image based on the existent image enhancement method. Histogram equalization is a simple and effective method of image enhancement in the spatial domain which describes an image of gray level content. Not only overall contrast of the fog-degraded image could be enhanced but also enhance the image edge details and texture property. We show that the combined method highlights the details of the fog-degraded image compared to traditional methods and also achieves a better result of the image clearness.

The primary concept used by the wavelet based image fusion is to extract the detail information from one image and use it for further analysis. The detail information in images is usually in the high frequency and wavelets have the ability to select the frequencies in both space and time. In subsequent chapter, segmentation of vessels in angiographic images using wavelet transform is addressed. For various visualization applications such as multi planar reformats or endovascular views, extraction of vessel centerline can be employed to generate particular visualization information. Vessel segmentation in X-ray angiographic frame is realized using Hessian-based vessel enhancement filters (HBVF) which have been proposed by Lorenz, Sato, and Frangi. HBVF is a powerful method for enhancing vascular structures in variety of imaging tasks. Angiographic image and its vesselness filtered version are fused using 2-D wavelet transform using pixel based average fusion rule to make an image which is used as a threshold for detecting the vessels.

Image fusion has become a common term used within medical diagnostics and treatment. The term is used when multiple patient images are registered and overlaid or merged to provide additional information. Fused images may be created from multiple images from the same imaging modality, or by combining information from multiple modalities, such as magnetic resonance image (MRI), computed tomography (CT), positron emission tomography (PET) etc. wavelet-based texture fusion of CT/MRI images. Wavelet transform is employed to extract energy and regional information entropy of texture features from images. In the process of fusion, we adopt the fusion rule of energy maximum for the wavelet low-frequency

coefficients; give the fusion rule according to the comparison of energy and regional information entropy contrast between CT/MRI images for the wavelet high frequency coefficients. Finally, we obtain the fused medical image via inverse wavelet transform.

The development of technology and networking has created serious threats to get secured data communication. This has resulted in research in the field of data security communication. One method of providing more security to data is information hiding. The information hiding schemes are principally classified into Steganography and Watermarking, according to the application. In the Steganography systems, transform domain technique (Wavelet Transform) is used to attain high capacity along with security and maintains the quality of the cover image which act as the key feature of this work. The objective for making steganographic encoding difficult to detect is to ensure that the changes to the carrier (the original signal) due to the injected payload (the signal to covertly embed) are visually (and ideally, statistically) negligible; that is to say, the changes are indistinguishable from the noise floor of the carrier.

2. WAVELET ANALYSIS

In conventional Fourier transform, we use sinusoids for basis functions. It can only provide the frequency information. Temporal information is lost in this transformation process. In some applications, we need to know the frequency and temporal information at the same time. Unlike conventional Fourier transform, wavelet transforms are based on small waves, called wavelets. It can be shown that we can both have frequency and temporal information by this kind of transform using wavelets. Moreover, images are basically matrices. For this reason, image processing can be regarded as matrix processing. Due to the fact that human vision is much more sensitive to small variations in color or brightness, that is, human vision is more sensitive to low frequency signals. Therefore, high frequency components in images can be compressed without distortion. Wavelet transform is one of a best tool for us to determine where the low frequency area and high frequency area is.

2.1 WAVELET

A wavelet is a wave-like oscillation with an amplitude that begins at zero, increases, and then decreases back to zero. It tends to irregular and unsymmetric and has an average value of zero.

$$\int_{-\infty}^{+\infty} \varphi(t) dt = 0 \quad (1)$$

The different types of wavelet are:

- **Haar:** Haar wavelet is a sequence of rescaled "square-shaped" functions. It is discontinuous, and resembles a step function.

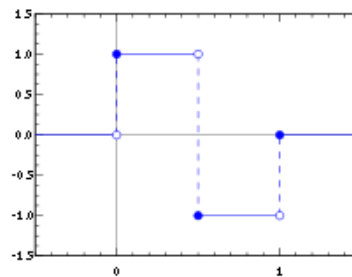


Fig. 2.1 Haar Wavelet

- **Daubechies:** The Daubechies wavelets, based on the work of Ingrid Daubechies, are a family of orthogonal wavelets defining a discrete wavelet transform and characterized by a maximal number of vanishing moments for some given support. The names of

the Daubechies family wavelets are written dbN, where N is the order, and db the "surname" of the wavelet.

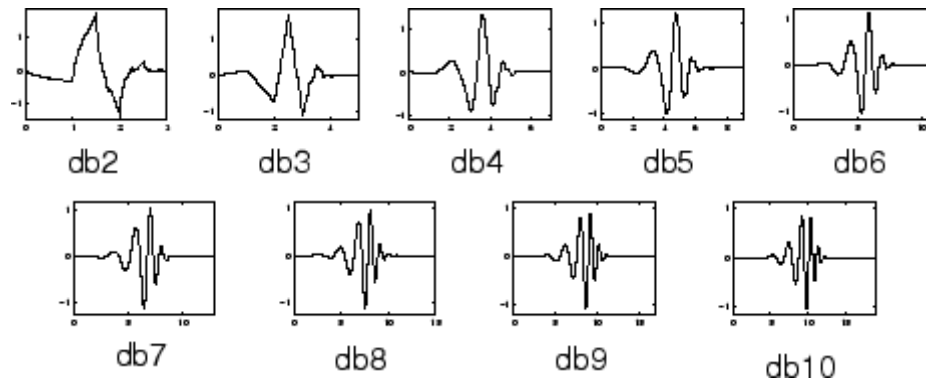


Fig. 2.2 The Daubechies family Wavelets

- **Mexican Hat:** This wavelet has no scaling function and is derived from a function that is proportional to the second derivative function of the Gaussian probability density function.

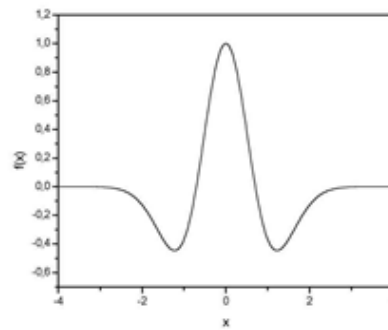


Fig. 2.3 Mexican Hat Wavelet

- **Biorthogonal:** This family of wavelets exhibits the property of linear phase, which is needed for signal and image reconstruction.

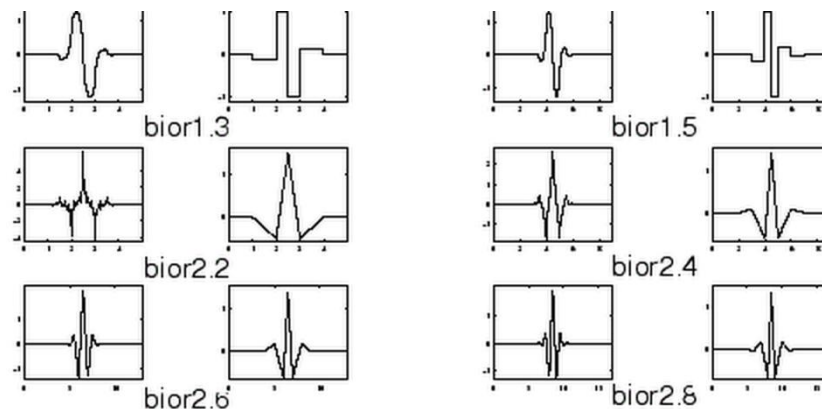


Fig. 2.4 The Biorthogonal family of Wavelets

- **Symlets:** The symlets are nearly symmetrical wavelets proposed by Daubechies as modifications to the db family. The properties of the two wavelet families are similar.

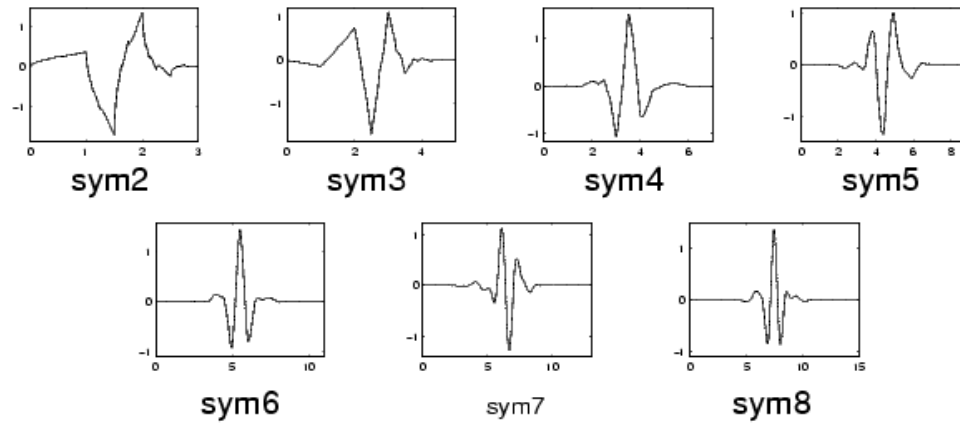


Fig. 2.5 The Symlets family of Wavelets

There are many other wavelets available like Gaussian derivatives, Morlet, Frequency B-Spline, Shannon etc.

2.2 CONTINUOUS WAVELET TRANSFORM (CWT)

The continuous wavelet transform (CWT) is defined as the sum over all time of the signal multiplied by scaled, shifted versions of the wavelet function, Ψ

$$W\{f(\mu, s)\} = \langle f, \varphi_{\mu, s} \rangle = \int_{-\infty}^{+\infty} f(t) \frac{1}{\sqrt{s}} \varphi^* \left(\frac{t-\mu}{s} \right) dt \quad (2)$$

where s = scale factor by which the wavelet is compressed or stretched

μ = time shifting factor by which the wavelet is advanced or delayed

Scale and Frequency: The higher scales correspond to the most "stretched" wavelets. The more stretched the wavelet, the longer the portion of the signal with which it is being compared, and thus the coarser the signal features being measured by the wavelet coefficients. Thus, there is a correspondence between wavelet scales and frequency as revealed by wavelet analysis:

- * Low scale $s \rightarrow$ Compressed wavelet \rightarrow Rapidly changing details \rightarrow High frequency
- * High scale $s \rightarrow$ Stretched wavelet \rightarrow Slowly changing, coarse features \rightarrow Low frequency

Steps for obtaining the Continuous Wavelet Transform(CWT) of a function:

1. Take a wavelet and compare it to a section at the start of the original signal.
2. Calculate a number, C , that represents how closely correlated the wavelet is with this section of the signal. The higher C is, the more the similarity. More precisely, if the

signal energy and the wavelet energy are equal to one, C may be interpreted as a correlation coefficient. Note that the results will depend on the shape of the wavelet you choose.

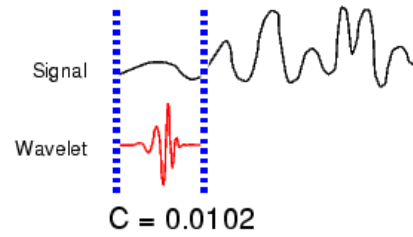


Fig. 2.6 Calculation of CWT

3. Shift the wavelet to the right and repeat steps 1 and 2 until you've covered the whole signal.

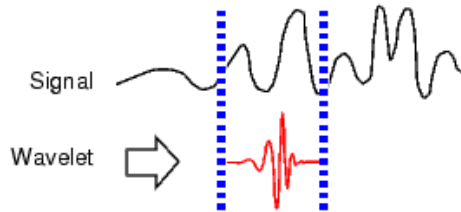


Fig. 2.7 Shifting Operation

4. Scale (stretch) the wavelet and repeat steps 1 through 3.

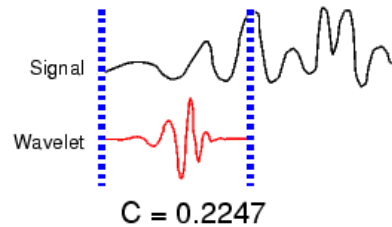


Fig. 2.8 Scaling Operation

5. Repeat steps 1 through 4 for all scales.

CWT can operate at every scale, from that of the original signal up to some maximum scale. The CWT is also continuous in terms of shifting: during computation, the analyzing wavelet is shifted smoothly over the full domain of the analyzed function.

2.3 DISCRETE WAVELET TRANSFORM (DWT)

The Discrete Wavelet Transform (DWT) is obtained if we choose scales and positions based on powers of two – the dyadic scales and positions. The analysis will be much more efficient and just as accurate. An efficient way to implement this scheme using filters was developed in 1988 by Mallat.

One Stage Filtering: Approximations and Details

For many signals, the low-frequency content is the most important part. It is what gives the signal its identity. The high-frequency content, on the other hand, imparts flavor or nuance. Consider the human voice. If you remove the high-frequency components, the voice sounds different, but you can still tell what's being said. However, if you remove enough of the low-frequency components, you hear gibberish.

In wavelet analysis, we often speak of approximations and details. The approximations are the high-scale, low-frequency components of the signal. The details are the low-scale, high-frequency components. The filtering process, at its most basic level, looks like this:

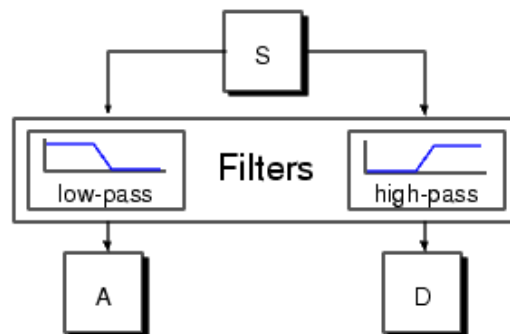


Fig. 2.9 Filtering Process

The original signal, S , passes through two complementary filters and emerges as two signals. Unfortunately, if we actually perform this operation on a real digital signal, we wind up with twice as much data as we started with. Hence, we do downsampling of the two signals obtained, A and D , and obtain the DWT coefficients, cA and cD .

The decomposition process can be iterated, with successive approximations being decomposed in turn, so that one signal is broken down into many lower resolution components. This is called the wavelet decomposition tree.

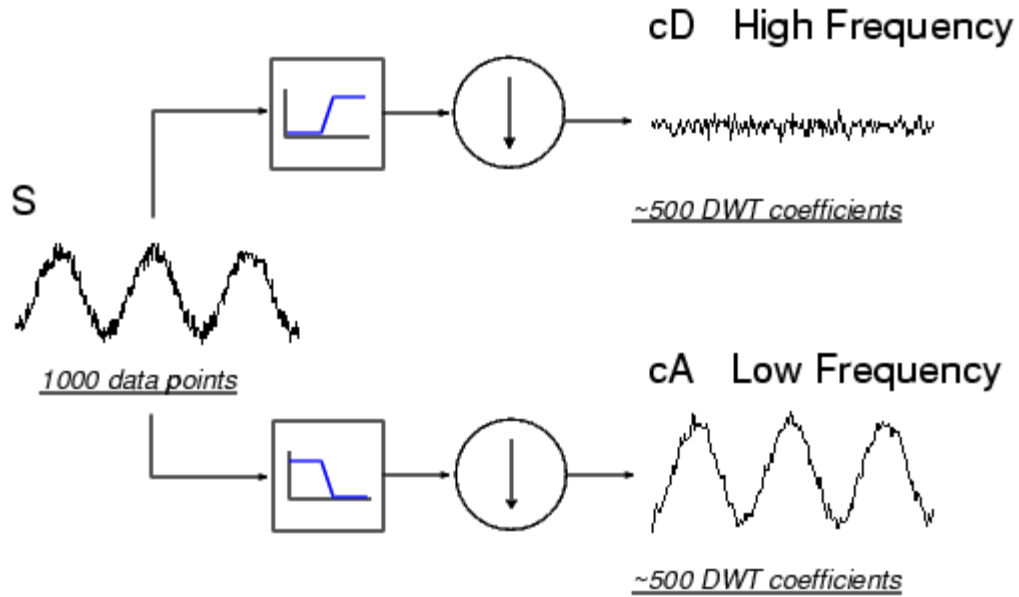


Fig. 2.10 Calculation of DWT coefficients

2.4. 2-D DISCRETE WAVELET TRANSFORM

The two dimensional wavelet transform is used to calculate the wavelet transform of matrices. It can also be used on images as an image is basically a matrix of pixel values. The algorithm for calculating 2-D DWT is similar to the one dimensional case. The following chart describes the basic decomposition steps for images:

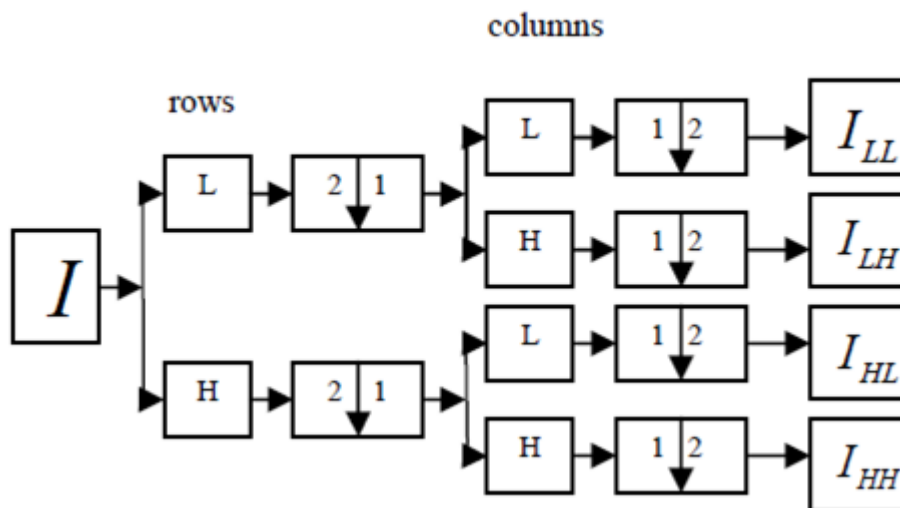


Fig. 2.11(a) Calculation of approximate and detailed coefficients of 2D DWT

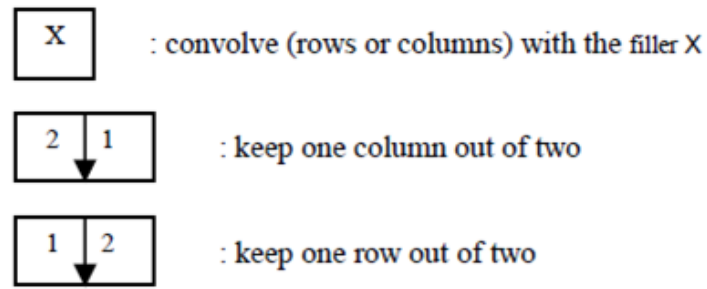


Fig. 2.11(b) Calculation of approximate and detailed coefficients of 2D DWT

The decomposition of a matrix or image leads to four components: one approximate component, (LL) and three details components in three orientations (LH,HL,HH) (horizontal, vertical, and diagonal). The decomposition process can be iterated, with successive approximations being decomposed in turn, so that one signal is broken down into many lower resolution components.

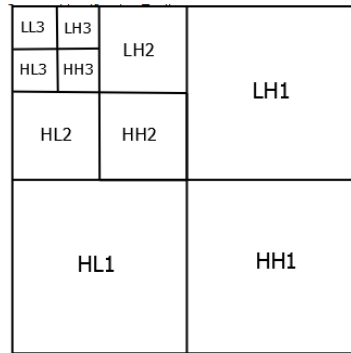


Fig. 2.12 3 Level Wavelet Image Decomposition

2.5 WAVELET RECONSTRUCTION

The process of obtaining the original signal from the approximation and detailed coefficients without loss of information is called wavelet reconstruction or inverse wavelet transform. Where wavelet analysis involves filtering and downsampling, the wavelet reconstruction process consists of upsampling and filtering. Upsampling is the process of lengthening a signal component by inserting zeros between samples.

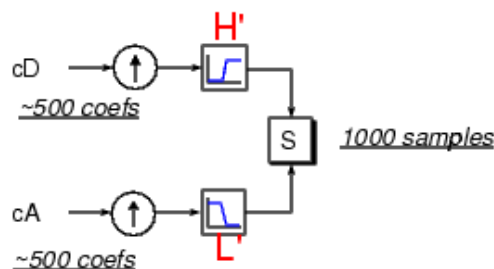


Fig. 2.13 Inverse Wavelet Transform

2.6 COMPARISON AMONG FOURIER TRANSFORM, SHORT-TIME FOURIER TRANSFORM (STFT) AND WAVELET TRANSFORM

Fourier transform convert signal in time domain to frequency domain by integrating over the whole time axis. But, it has a serious drawback. In transforming to the frequency domain, time information is lost. When looking at a Fourier transform of a signal, it is impossible to tell when a particular event took place.

In an effort to correct this deficiency, Dennis Gabor (1946) adapted the Fourier transform to analyze only a small section of the signal at a time -- a technique called windowing the signal. Gabor's adaptation, called the **Short-Time Fourier Transform (STFT)**, maps a signal into a two-dimensional function of time and frequency. While the STFT compromise between time and frequency information can be useful, the drawback is that once you choose a particular size for the time window, that window is the same for all frequencies.

Wavelet Transform represents the next logical step: a windowing technique with variable-sized regions. Wavelet analysis allows the use of long time intervals where we want more precise low-frequency information, and shorter regions where we want high-frequency information. It does not use a time-frequency region, but rather a time-scale region. One major advantage afforded by wavelets is the ability to perform local analysis - that is, to analyze a localized area of a larger signal.

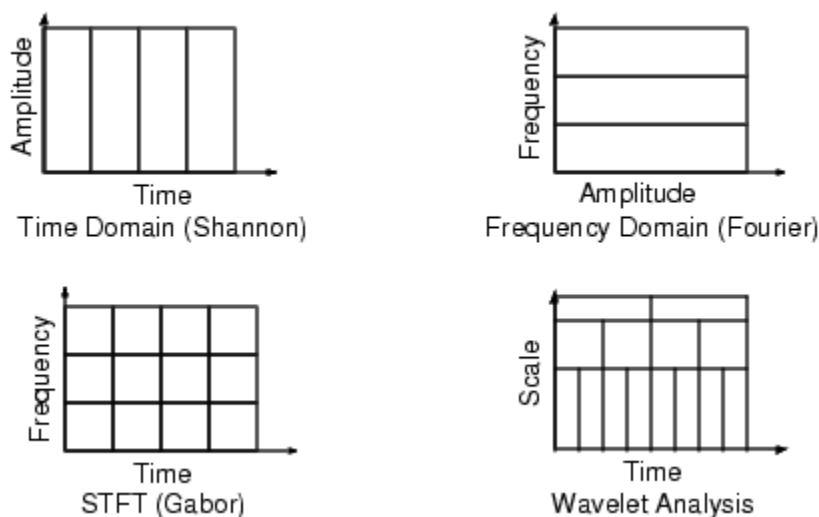


Fig. 2.14 Comparison among Fourier Transform, Short Time Fourier Transform and Wavelet Transform

2.7 APPLICATIONS OF WAVELETS

Wavelets are a powerful statistical tool which can be used for a wide range of applications, namely

- Signal processing
- Data compression
- Smoothing and image denoising
- Fingerprint verification
- Biology: for cell membrane recognition, to distinguish the normal from the pathological membranes
- DNA analysis, protein analysis
- Blood-pressure, heart-rate and ECG analyses
- Finance (which is more surprising), for detecting the properties of quick variation of values
- In Internet traffic description, for designing the services size
- Industrial supervision of gear-wheel
- Speech recognition
- Computer graphics and multifractal analysis

Wavelets have been used successfully in other areas of geophysical study. Orthonormal wavelets, for instance, have been applied to the study of atmospheric layer turbulence. Wavelets have also been used to analyze seafloor bathymetry or the topography of the ocean floor.

2.8 WAVELET TOOLBOX

The Wavelet Toolbox is a collection of functions built on the MATLAB Technical Computing Environment. It provides tools for the analysis and synthesis of signals and images using wavelets and wavelet packets within the framework of MATLAB.

The toolbox provides two categories of tools:

- Command line functions
- Graphical interactive tools

The first category of tools is made up of functions that one can call directly from the command line or from one's own applications. Most of these functions are M-files, series of statements that implement specialized wavelet analysis or synthesis algorithms. One can view the code for these functions using the following statement:

```
type function_name
```

A summary list of the Wavelet Toolbox functions is available typing

```
help wavelet
```

The second category of tools is a collection of graphical interface tools that afford access to extensive functionality. One can access these tools by typing

```
wavemenu
```

from the command line

2.8.1 DWT & IDWT

Two of the most important functions for wavelet analysis are `dwt` and `idwt` which are used to calculate wavelet transform and inverse wavelet transform respectively of a signal. For 2 dimensional signals i.e. images, we use the commands `dwt2` and `idwt2`. `dwt` calculates the approximation and detailed coefficients of the signal using the specified wavelet. `idwt` uses the approximate and detailed coefficients to recover the signal back in time domain.

2.8.2 Wavelet Families

There are different types of wavelet families whose qualities vary according to several criteria. The main criteria are:

- The support of ψ , and ϕ , the speed of convergence at infinity to 0 of these functions when the time or the frequency goes to infinity, which quantifies both time and frequency localizations.
- The symmetry, which is useful in avoiding dephasing in image processing.
- The number of vanishing moments for ψ or for ϕ (if it exists), which is useful for compression purpose.
- The regularity, which is useful for g

These are associated with two properties that allow fast algorithm and space-saving coding:

- The existence of a scaling function ϕ .
- The orthogonality or the biorthogonality of the resulting analysis,

The ϕ and ψ functions can be computed using **wavefun**

The filters are generated using **wfilters**

The table below outlines the wavelet families included in the toolbox

MATLAB Function	Wavelet Name
morl	Morlet
mexh Mexican hat	Mexican Hat
meyr	Meyer
haar	Haar
dbN	Daubechies
symN	Symlets
coifN	Coiflets
biorNr.Nd	Splines biorthogonal wavelets

Table 2.1 Wavelet families in the toolbox

3. TEXTURE CLASSIFICATION

In many machine vision and image processing algorithms, simplifying assumptions are made about the uniformity of intensities in local image regions. However, images of real objects often do not exhibit regions of uniform intensities. For example, the image of a wooden surface is not uniform but contains variations of intensities which form certain repeated patterns called visual texture. The patterns can be the result of physical surface properties such as roughness or oriented strands which often have a tactile quality, or they could be the result of reflectance differences such as the colour on a surface.

The textural patterns or structures mainly result from the physical surface properties, such as roughness or oriented structured of a tactile quality. It is widely recognized that a visual texture, which can easily perceive, is very difficult to define. The difficulty results mainly from the fact that different people can define textures in applications dependent ways or with different perceptual motivations, and they are not generally agreed upon single definition of texture. The development in multi-resolution analysis such as Gabor and wavelet transform help to overcome this difficulty.



Fig. 3.1 Different textures in real world

In this chapter, it describes that, texture classification using Wavelet Statistical Features (WSF), Wavelet Co-occurrence Features (WCF) and to combine both the features namely Wavelet Statistical Features and Wavelet Co-occurrence Features of wavelet transformed images with different feature databases can results better. And further the Features are analysed introducing Noise (Gaussian, Poisson, Salt n Paper and Speckle) in the image to be classified. The result suggests that the efficiency of Wavelet Statistical Feature is higher in classification even in noise as compared to other Features efficiency.

The texture classification process has been divided into 3 phases which are:

1. Wavelet Transform of image
2. Texture Training
3. Texture classification

3.1 WAVELET TRANSFORM OF IMAGE

The image is decomposed into four sub-bands and critically sub-sampled by applying DWT2. The `dwt2` command performs single-level two-dimensional wavelet decomposition with respect to either a particular wavelet. Here we have used the `db1` wavelet.

These sub-bands labelled LH1, HL1 and HH1 represent the finest scale wavelet coefficients i.e., detail images while the sub-band LL1 corresponds to coarse level coefficients i.e., approximation image. To obtain the next coarse level of wavelet coefficients, the sub-band LL1 alone is further decomposed and critically sampled. This results in two-level wavelet decomposition.

The values or transformed coefficients in approximation and detail images (sub-band images) are the essential features, which are useful for texture analysis and discrimination.

As micro-textures or macro-textures have non-uniform gray level variations, they are statistically characterized by the features in approximation and detail images. The values in the sub-band images or their combinations or the derived features from these bands uniquely characterize a texture. The features obtained from these wavelet transformed images are used for texture analysis, namely, classification.

3.2 TEXTURE TRAINING

In texture training the Wavelet Statistical features (WSF) and the Wavelet co-occurrence features (WCF) are calculated.

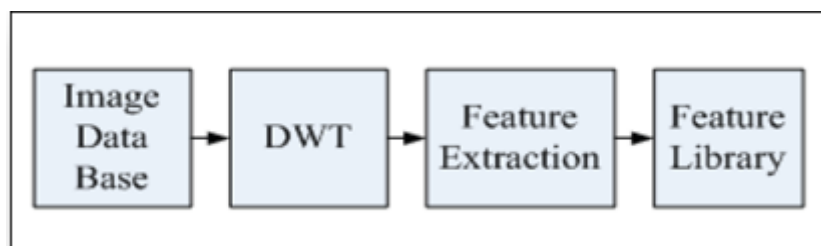


Fig 3.2 Texture training

3.2.1 Wavelet Statistical Features

For the Wavelet Statistical features (WSF) training, the known texture images are decomposed using DWT. Then, mean and standard deviation of approximation and detail sub-bands of decomposed images are calculated and are stored in the feature library.

Mean is calculated using the formula:

$$Mean(m) = \frac{1}{N^2} \sum_{i=1}^N \sum_{j=1}^N p(i,j) \quad (3)$$

Standard Deviation is calculated using:

$$SD(\sigma) = \sqrt{\frac{1}{N^2} \sum_{i=1}^N \sum_{j=1}^N [p(i,j) - m]^2} \quad (4)$$

Where $p(i,j)$ is the transformed value in i and j for any $N \times N$ sub band.

3.2.2 Wavelet Co-occurrence Features

In order to improve the correct classification rate further, it is proposed to find co-occurrence matrix features for original image, approximation and detail sub-bands of 1-level DWT decomposed images (i.e., LL1, LH1, HL1 and HH1).

The various co-occurrence features such as contrast, energy, entropy, local homogeneity are calculated from the co-occurrence matrix $C(i; j)$.

- Contrast: $\sum |i - j|^2 p(i, j)$
- Correlation: $\sum \frac{(i - \mu_i)(j - \mu_j)p(i, j)}{\sigma_i \sigma_j}$
- Energy: $\sum p(i, j)^2$
- Homogeneity: $\sum p(i, j) / (1 + |i - j|)$

3.3 TEXTURE CLASSIFICATION

The unknown texture is decomposed using DWT and a similar set of wavelet statistical and co-occurrence matrix features are extracted and compared with the corresponding feature values stored in the features library using distance vector formula.

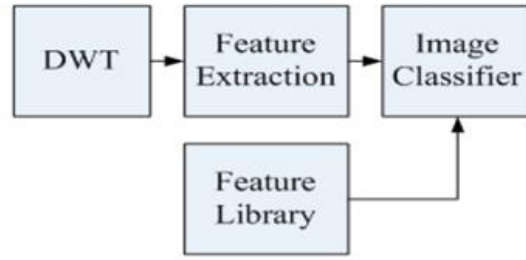


Fig 3.3 Texture Classification

The unknown texture is decomposed using DWT and a similar set of wavelet statistical and co-occurrence matrix features are extracted and compared with the corresponding feature values stored in the features library using distance vector formula given as:

$$D(i) = \sum_{j=1}^{No.of\ feature} f_j(x) - f_j(i) \quad (5)$$

Where, $f_j(x)$ represents the features of unknown texture while $f_j(i)$ represents the features of known i th texture in the library. Then, the unknown texture is classified as i th texture, if the distance is minimum among all textures, available in the library. The sum of the absolute value of the difference between the two feature vectors is calculated.

3.4 NOISE INTRODUCTION

If noise is introduced in the image to be classified, the proposed method still classifies correctly. The features of noisy images are compared with the features of the images stored in database. The noise is introduced in image and it shows the best feature that is immune to noise is Wavelet Statistical Feature. The Gaussian noise, Poisson noise, Salt n Paper and Speckle noise is introduced in the image that is to be classified but the classification is correct at 100 % if the F1 features which is Wavelet Statistical Feature. This suggests that WSF gives correct features of noisy images also.

The image is kept at classification side and noise is introduced and at database also same image is kept. The features are compared and hence WSF gives minimum deviation when compared with the non-noisy image with database. The rest features takes noise as features and classifies noisy images.

3.5 ALGORITHM

1. Take 9 images of different textures, aluminium foil, brown bread, sponge, orange peel, linen, cracker, cotton, foam and sandpaper, and store them in the library as texture database.

2. Compute the 2D Discrete Wavelet Transform of these nine images and obtain the corresponding approximation and detailed coefficients sub images.
3. Calculate mean, standard deviation and entropy of these sub images and energy, contrast, correlation and homogeneity of the co-occurrence matrix of the sub images. Store these features of each image in a feature matrix.
4. Read the test image whose texture has to be identified.
5. Compute 2D Discrete Wavelet Transform of the test image and obtain the corresponding approximation and detailed coefficients sub images.
6. Calculate mean, standard deviation and entropy of the test image and energy, contrast, correlation and homogeneity of the co-occurrence matrix of the test image. Store these features of the test image in a feature matrix
7. Subtract the feature matrix of the test image from feature matrix of each of the 9 images in database to calculate the distance between them. Take the absolute value of the distance.
8. Find the image whose distance is minimum from the test image. Hence, the test image is classified as belonging to that texture.

3.6 RESULT & DISCUSSION

MATLAB R2008.0 has been used for simulations and demonstration of the proposed idea. 9 images of different textures, sponge, sandpaper, orange peel, linen, cracker, cotton, foam, brown bread and aluminium foil are taken and stored and their feature vector calculated. The test image's feature vector is also calculated and is compared with each of the feature vector of database images to classify the unknown texture. The test image is successfully classified as sponge. Afterwards, noise is also introduced in the image but we get the correct classification.

Database Images:

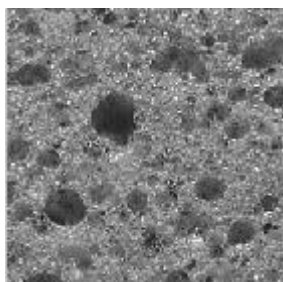


Fig. 3.4 Sponge

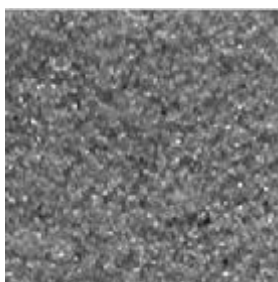


Fig. 3.5 Sandpaper

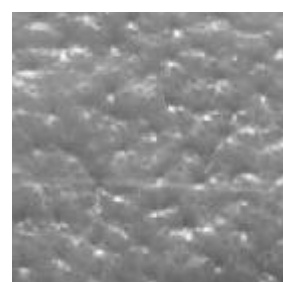


Fig. 3.6 Orange Peel

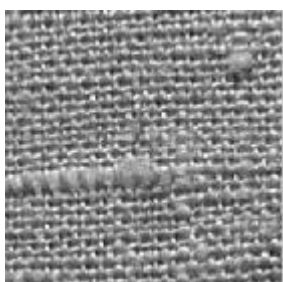


Fig. 3.7 Linen

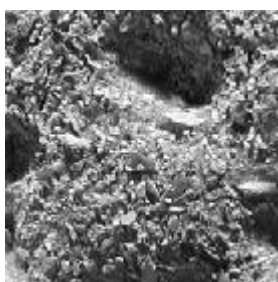


Fig. 3.8 Cracker

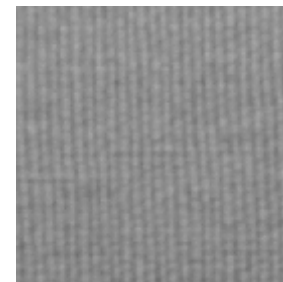


Fig. 3.9 Cotton

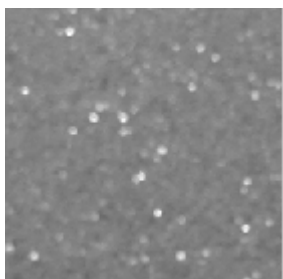


Fig. 3.10 Foam

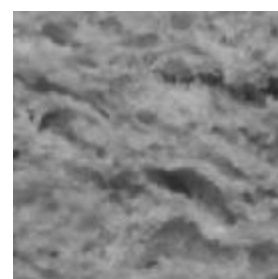


Fig. 3.11 Brown Bread



Fig. 3.12 Aluminium Foil

Test Images:

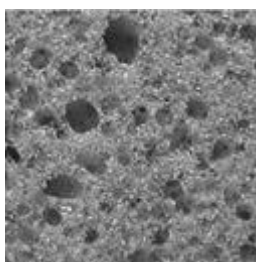


Fig. 3.13 Test Image

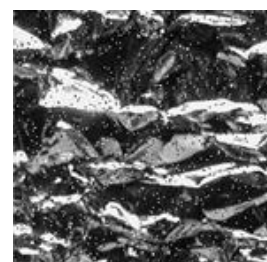


Fig. 3.14 Image with
Salt and Pepper noise

3.7 FUTURE APPLICATIONS

The research results will have a wide range of useful applications, including but not restricted to human face image recognition, medical and biological imaging and knowledge discovery, advanced image and video compression algorithms, and content-based image indexing and retrieval.

The differences between the textures of healthy and unhealthy tissues can be found out.

In satellite images texture can be employed to differentiate terrains such as forests, buildings and sea.

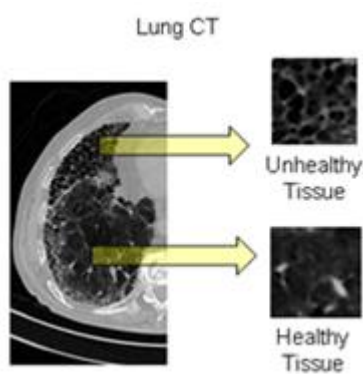


Fig. 3.15 Application in CT scan

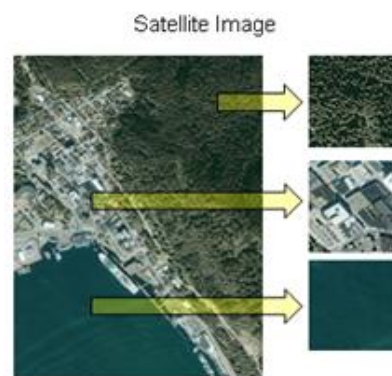


Fig 3.16 Application in satellite image

4. IMAGE FUSION

Image fusion is the process by which two or more images are combined into a single image retaining the important features from each of the original images. The fusion of images is often required for images acquired from different instrument modalities or capture techniques of the same scene or objects. Important applications of the fusion of images include medical imaging, microscopic imaging, remote sensing, computer vision, and robotics. One can use the following four examples to illustrate the purpose of image fusion:

1. In optical remote sensing fields, the multispectral (MS) image which contains color information is produced by three sensors covering the red, green and blue spectral wavelengths. Because of the trade-off imposed by the physical constraint between spatial and spectral resolutions, the MS image has poor spatial resolution. On the contrast, the panchromatic (PAN) images has high spatial resolution but without color information. Image fusion can combine the PAN image and the MS image.

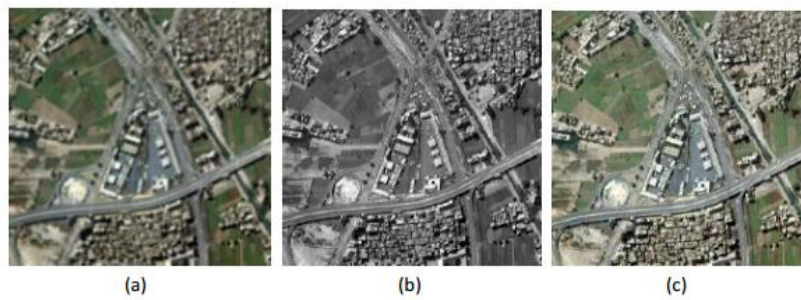


Fig. 4.1 Image fusion for an IKONOS scene for Cairo, Egypt: (a) multispectral low resolution input image, (b) panchromatic high resolution input image, and (c) fused image of IHS.

2. As the optical lenses in CCD devices have limited depth-of focus, it is often impossible to obtain an image in which all relevant objects are in focus. To achieve all interesting objects in focus, several CCD images, each of which contains some part of the objects in focus, are required. The fusion process is expected to select all focused objects from these images.

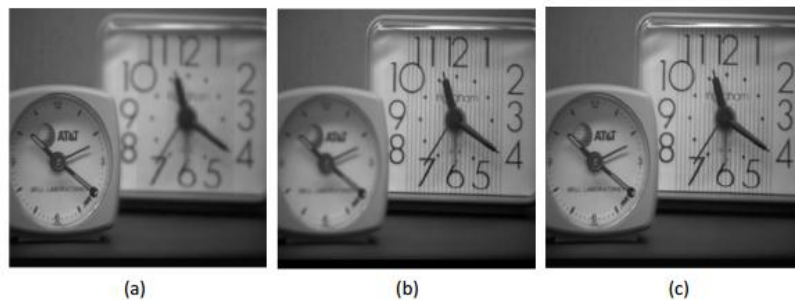


Fig. 4.2 CCD visual images with the (a) right and (b) left clocks out of focus, respectively; (c) the resulting fused image from (a) and (b) with the two clocks in focus.

3. Sometimes the “in focus” problem is due to the different characteristics of different types of optical sensors, such as visual sensors, infrared sensors, Gamma sensors and X-Ray sensors. Each of these types of sensors offers different information to the human operator or a computer vision system. The image fusion process can combine all the interesting details into a composite image.

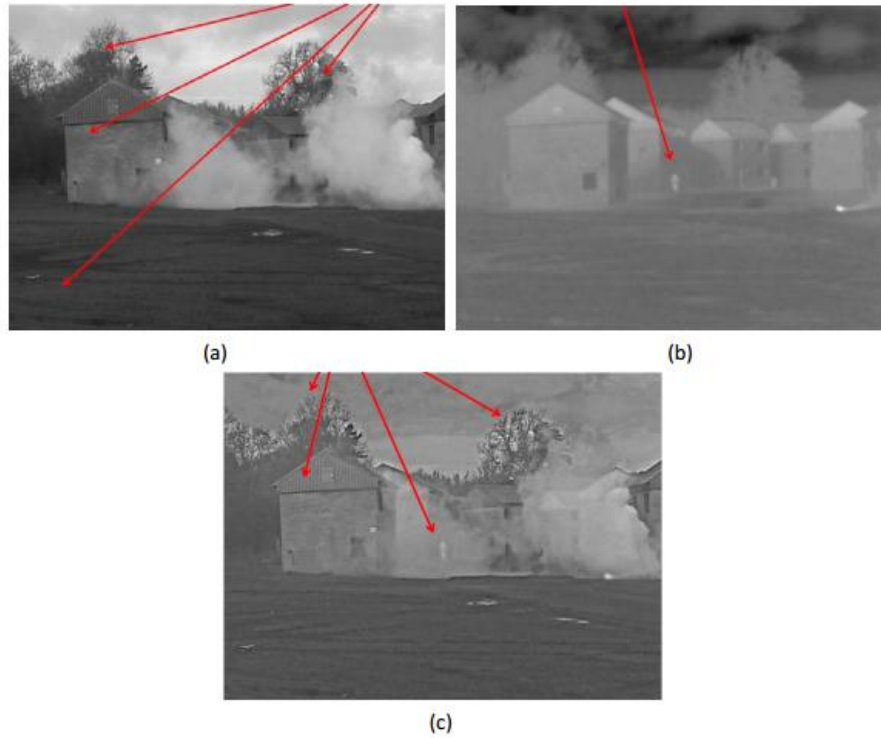


Fig. 4.3 Images captured from the (a) visual sensor and (b) infrared sensor, respectively; (c) the resulting fused image from (a) and (b) with all interesting details in focus.

4. In medical imaging, different medical imaging techniques may provide scans with complementary and occasionally conflicting information, such as magnetic resonance image (MRI), computed tomography (CT), positron emission tomography (PET), and single photon emission computed tomography (SPECT). The object of image fusion is to achieve a high spatial resolution image with functional and anatomical information.

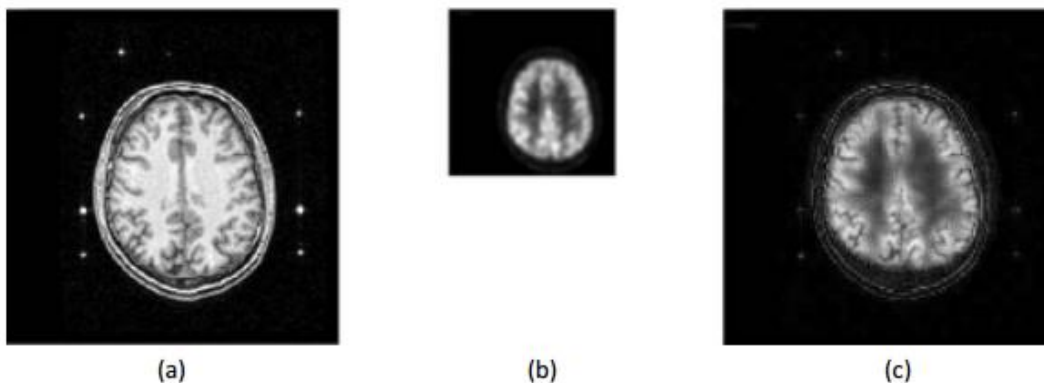


Fig. 4.4 (a) MRI and (b) PET images; (c) fused image from (a) and (b).

4.1 IMAGE FUSION METHODS

Fusion techniques include the simplest method of pixel averaging to more complicated methods such as principal component analysis and wavelet transform fusion. Several approaches to image fusion can be distinguished, depending on whether the images are fused in the spatial domain or they are transformed into another domain, and their transforms fused. There are various methods that have been developed to perform image fusion. Some well-known image fusion methods are listed below:

1. Intensity-hue-saturation (IHS) transform based fusion
2. Principal component analysis (PCA) based fusion
3. Arithmetic combinations
4. Multiscale transform based fusion
 - i) High-pass filtering method
 - ii) Pyramid method
 - iii) Wavelet transform
 - iv) Curvelet transform
5. Total probability density fusion
6. Biologically inspired information fusion

4.2 WAVELET BASED IMAGE FUSION

The standard image fusion techniques, such as IHS based method, PCA based method and Brovey transform method operate under spatial domain. However, the spatial domain fusions may produce spectral degradation. This is particularly crucial in optical remote sensing if the images to fuse were not acquired at the same time. Therefore, compared with the ideal output of the fusion, these methods often produce poor result. As multi resolution analysis has become one of the most promising methods in image processing, the wavelet transform has become a very useful tool for image fusion. It has been found that wavelet-based fusion techniques outperform the standard fusion techniques in spatial and spectral quality, especially in minimizing color distortion.

In common with all transform domain fusion techniques the transformed images are combined in the transform domain using a defined fusion rule then transformed back to the spatial domain to give the resulting fused image. Wavelet transform fusion is more formally defined by considering the wavelet transforms Ψ of the two registered input images $I_1(x,y)$ and $I_2(x,y)$ together with the fusion rule Φ . Then, the inverse wavelet transform Ψ^{-1} is computed, and the fused image $I(x,y)$ is reconstructed.

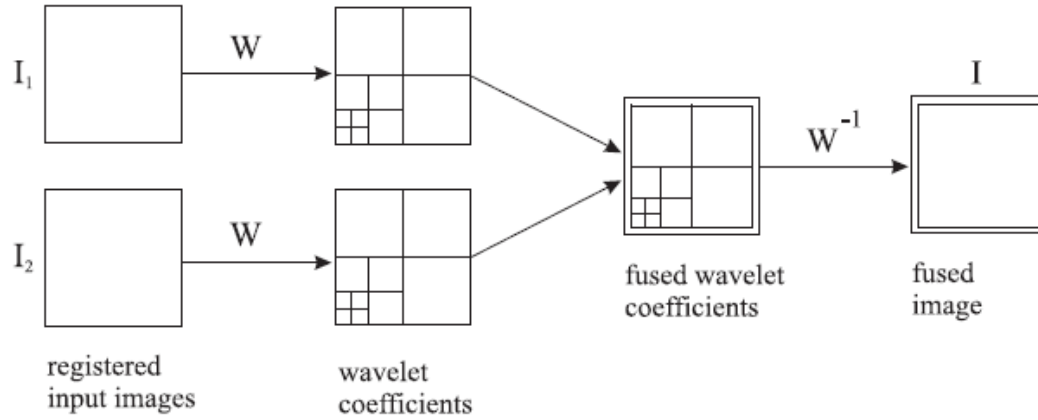


Fig. 4.5 Fusion of the wavelet transforms of two images

Three fusion rule schemes using discrete wavelet transform based image fusion are:

- **Maximum Selection (MS) scheme:** This simple scheme just picks the coefficient in each sub band with the largest magnitude.
- **Weighted Average (WA) scheme:** This scheme uses a normalised correlation between the two images' sub bands over a small local area. The resultant coefficient for reconstruction is calculated from this measure via a weighted average of the two images' coefficients.
- **Window Based Verification (WBV) scheme:** This scheme creates a binary decision map to choose between each pair of coefficients using a majority filter.

5. FOG–DEGRADED IMAGE ENHANCEMENT

One of the major reasons for accidents in air, on sea and on the road is poor visibility due to presence of fog or mist in the atmosphere. Fog produces whitening effect, will cause the image to degenerate, even fuzzy, which will bring the serious influence for the transportation system and the outdoors vision system. Therefore, it has very vital practical significance for strengthening the contrast gradient and the image detail information from the fog-degraded image. Now, there are mainly two kinds of fog-degraded image clearness processing technologies. One is the physical model based on degraded image restoration method, which carries on modelling analysis and recovers scene from the view of physical causes to the action of atmospheric scattering, needed to capture the same scene under different weather conditions in the two images to estimate the scene depth information, obviously, it is very difficult to realize in some situations.

Another one is from the perspective of image processing to enhance image contrast, which achieves the purpose of image clearness. Fast wavelet transform is used to fog-degraded image decomposition based on the existent traditional histogram equalization in this chapter which is according to the characteristics of fast wavelet transform, and the high frequency part of image is processed by non-linear operator. Not only overall contrast of the fog-degraded image could be enhanced but also enhance the image edge details and texture property. The chapter shows that the combined method highlights the details of the fog-degraded image compared to traditional methods and also achieves a better result of the image clearness.

5.1 HOMOMORPHIC FILTERING

5.1.1 General Overview

It is a generalized technique for signal and image processing, involving a nonlinear mapping to a different domain in which linear filter techniques are applied, followed by mapping back to the original domain.

In this chapter, we are using it for image enhancement. Homomorphic filter simultaneously normalizes the brightness across an image and increases contrast. Here homomorphic filtering is used to remove multiplicative noise. Illumination and reflectance are not separable, but their approximate locations in the frequency domain may be located. Since illumination and reflectance combine multiplicatively, the components are made additive by taking the logarithm of the image intensity, so that these multiplicative components of the image can be

separated linearly in the frequency domain. Illumination variations can be thought of as a multiplicative noise, and can be reduced by filtering in the log domain.

To make the illumination of an image more even, the high-frequency components are increased and low-frequency components are decreased, because the high-frequency components are assumed to represent mostly the reflectance in the scene (the amount of light reflected off the object in the scene), whereas the low-frequency components are assumed to represent mostly the illumination in the scene. That is, high-pass filtering is used to suppress low frequencies and amplify high frequencies, in the log-intensity domain.

5.1.2 Detailed Steps

- Homomorphic filtering is one such technique for removing multiplicative noise that has certain characteristics. Homomorphic filtering is used for correcting non-uniform illumination in images. The illumination-reflectance model of image formation says that the intensity at any pixel, which is the amount of light reflected by a point on the object, is the product of the illumination of the scene and the reflectance of the object(s) in the scene, i.e.,

$$I(x,y)=L(x,y) R(x,y) \quad (6)$$

where I is the image, L is scene illumination, and R is the scene reflectance. Reflectance R arises from the properties of the scene objects themselves, but illumination L results from the lighting conditions at the time of image capture. To compensate for the non-uniform illumination, the key is to remove the illumination component L and keep only the reflectance component R .

- Illumination typically varies slowly across the image as compared to reflectance which can change quite abruptly at object edges. This difference is the key to separating out the illumination component from the reflectance component. In homomorphic filtering we first transform the multiplicative components to additive components by moving to the log domain.

$$\ln(I(x,y)) = \ln(L(x,y) R(x,y)) \quad (7)$$

$$\ln(I(x,y)) = \ln(L(x,y)) + \ln(R(x,y)) \quad (8)$$

- Then we use a high-pass filter in the log domain to remove the low-frequency illumination component while preserving the high-frequency reflectance component. We can do high-pass filtering in either the spatial or the spectral domain. There are different types of high-pass filters you can construct, such as Gaussian, Butterworth,

and Chebychev filters. In frequency domain the homomorphic filtering process looks like:

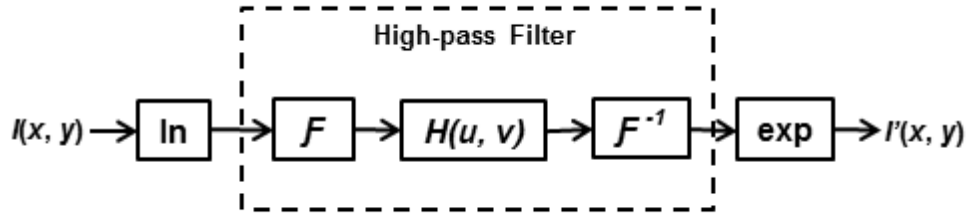


Fig. 5.1 Homomorphic filtering in frequency domain

5.2 HISTOGRAM EQUALIZATION

5.2.1 General Overview

Histogram equalization is a simple and effective method of image enhancement in the spatial domain which describes an image of gray level content. The basic principle of histogram equalization is that broadens the gray value of image in playing a major role, merge the gray value which can not afford a major role on the image, so as to achieve a clear image purposes. Traditional histogram equalization acts on the image of fog, which cause to enhance the image contrast, and clear the fog-degraded image. But it also has following disadvantages, the transformed image reduces in some details of the part of the definition, some area have been enhanced, and prone to excessive due to the contrast of gradation resulting distortion, present the foggy image noise to be strengthened and so on.

5.2.2 Implementation

Consider a discrete grayscale image $\{x\}$ and let n_i be the number of occurrences of gray level i . The probability of an occurrence of a pixel of level i in the image is

$$p_x(i) = p(x = i) = \frac{n_i}{n}, \quad 0 \leq i < L \quad (9)$$

L being the total number of gray levels in the image (typically 256), n being the total number of pixels in the image, and $p_x(i)$ being in fact the image's histogram for pixel value i , normalized to $[0,1]$.

Let us also define the cumulative distribution function corresponding to p_x as

$$cdf_x(i) = \sum_{j=0}^i p_x(j) \quad (10)$$

which is also the image's accumulated normalized histogram.

We would like to create a transformation of the form $y = T(x)$ to produce a new image $\{y\}$, with a flat histogram. Such an image would have a linearized CDF across the value range, i.e.

$$cdf_y(i) = iK \quad (11)$$

for some constant K . The properties of the CDF allow us to perform such a transform (see Inverse distribution function); it is defined as

$$cdf_y(y') = cdf_y(T(k)) = cdf_x(k) \quad (12)$$

where k is in the range $[0, L)$. Notice that T maps the levels into the range $[0, 1]$, since we used a normalized histogram of $\{x\}$. In order to map the values back into their original range, the following simple transformation needs to be applied on the result:

$$y' = y \cdot (\max\{x\} - \min\{x\}) + \min\{x\} \quad (13)$$

5.3 WAVELET FUSION METHOD ANALYSIS

Because the wavelet multi-resolution analysis has good spatial and frequency domain localization features, it can focus on any of the details of image, analyze and highlight details, and can also lower noise, so the methods which combine both histogram equalization and wavelet transform are used in this chapter. Not only wavelet fusion method can enhance contrast of the fog-degraded image, but also highlight image details and reduce noise. The model which combines both non-linear gain methods based on wavelet transform and histogram equalization is Wavelet Fusion Model.

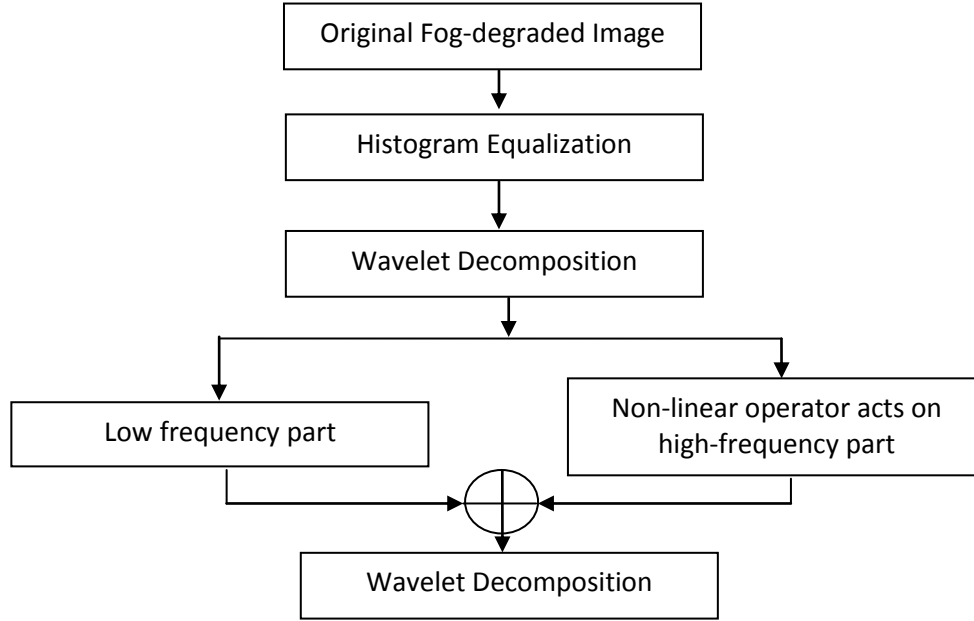


Fig. 5.2 Wavelet Fusion Model

5.4 NON-LINEAR GAIN FUNCTION

As more details of the image concentrate in the high frequency sub-band. So to achieve the result of enhancing the foggy image, we take detail part. Non-linear Gain Function can do enhanced modification by means of transforming to the detail coefficients which are obtained by wavelet decomposition. Therefore, the selection of gain function influences the enhanced effect directly. According to treated fog-degraded image, this chapter adopts non-linear gain function given as follows :-

$$f(x) = a[\text{sigm}(c(x - b)) - \text{sigm}(-c(x + b))] \quad (14)$$

In this expression,

$$a = \frac{1}{\text{sigm}(c(1-b)) - \text{sigm}(-c(1+b))} \quad (15)$$

$$\text{sigm}(x) = \frac{1}{1+e^{-x}} \quad (16)$$

where, $0 < b < 1$, b and c are parameters which are used in controlling the enhanced range and gain intensity. The curve of $f(x)$ is showed by fig.5.3.

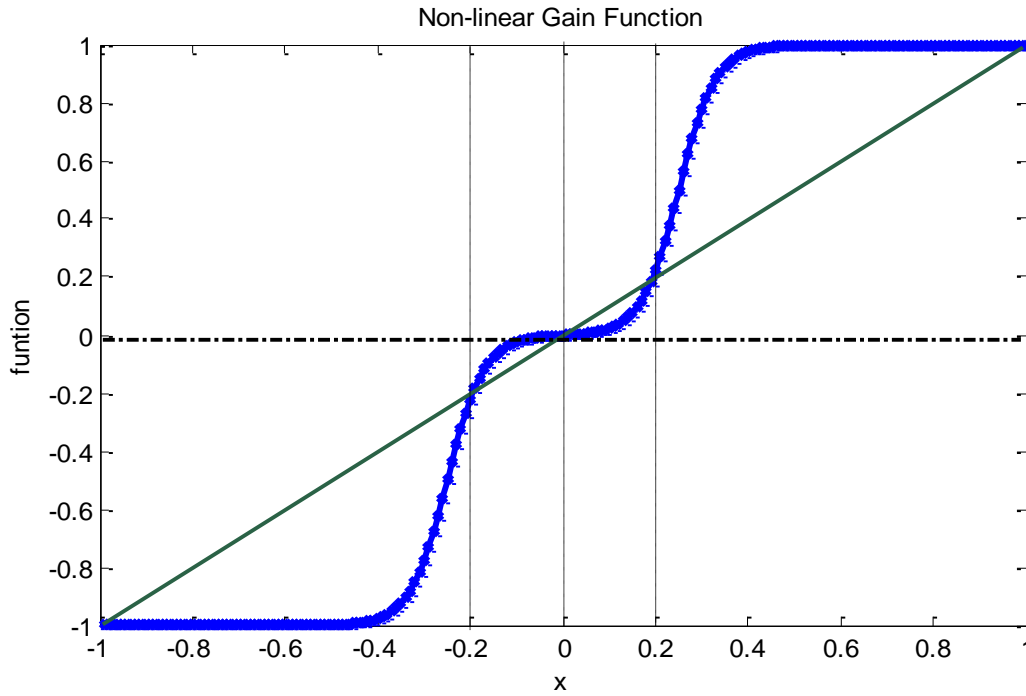


Fig. 5.3 The curve of $f(x)$ when $b = 0.25$ and $c = 25$

It is showed that $f(x)$ is a monotone increasing function in $[-1,1]$. The enhanced function mainly enlarges coefficients of the absolute values, the smaller coefficients are generally believed noise components which needed to restrain, and the larger coefficients correspond to the clear edge of image which need to strengthen. In other words, there is always a threshold value which is reduced when the coefficient is less than T and increased when more than T . At the same time the gain function also restrains distortion phenomenon to happen among the two endpoints.

Before the computation, the transform coefficients are necessary in normalization processing. The *enhanced function* is showed by the following expression.

$$f(x) = ax_{max}[\text{sigm}(c(x/x_{max} - b)) - \text{sigm}(-c(x/x_{max} + b))] \quad (17)$$

Meanwhile, the threshold value can be calculated by the following expression.

$$T_j^i = \frac{1}{2} \sqrt{\frac{1}{MN} \sum_{m=1}^M \sum_{n=1}^N (y_j^i(m,n) - \text{mean}_y)^2} \quad (18)$$

Among them, y_j^i is the i th sub-band coefficient of the j th layer, and mean_y is the mean of sub-band.

5.5 ALGORITHM

The contrastive test mainly apply programming software such as MATLAB.

- Initialize the original fog-degraded image (de-noising or modify the data type of image matrix are used to enhance the accuracy).
- Apply Homomorphic filtering on fog-degraded image to simultaneously normalize the brightness across an image and increase contrast.
- Apply Histogram equalization to enhance the image contrast and clear the fog-degraded image.
- Do Wavelet decomposition to get approximation and detail coefficients of histogram equalized image, while determine the threshold value and corresponding enhancement operator.
- Enhancement operator is used to process the wavelet transform coefficients adaptively, while obtain the high frequency details of the corresponding image.
- Reconstruct the image by applying inverse discrete wavelet transform.
- The reconstructed image is fog-degraded enhanced image, i.e. required image.

5.6 RESULT AND DISCUSSION



(a). Original Image



(b). Homomorphic Filtered Image



(c). Histogram Equalized Image



(d). Wavelet Fused Image

Fig.5.4 The results of the contrastive test

According to fig.5.4, it could obtain conclusion as follows. The effect is not obvious after homomorphic filtering process through comparing with fig.5.4(a) and (b). As is revealed in fig.5.4(c), after the histogram equalization processing fog-degraded image's contrast gradient strengthens obviously, the image becomes quite clear but presents over enhancement which has caused image partial content distortion and changed of image edge detail. Likewise, in the fig.5.4(d), the method of this chapter has avoided the distorted phenomenon of enhanced image contrast gradient by the histogram equalizing, and better enhanced image edge detail and the texture characteristic has achieved the purpose of clearing fog-degraded image.

The above section carried on the analysis of enhancement effect from the subjective angle, and then mainly compares the experimental results from the image clarity objectively. The image definition refers to light and shadow levels especially weather clearness among the tiny levels of light and shadow contrast, and the higher image definition express the more image local feature and detail information are contained. There are many evaluation functions of the image definition, the chapter mainly utilize squared gradient function which evaluates the experimental results objectively, and the quantitative comparison results are showed.

Image	(a)	(b)	(c)	(c)
Gradient($\times 10^6$)	7.26	51.3	57.2	106.2

Table.5.1 Quantitative analysis of results of Fig.5.4

The gradient refers to the module value in the table 5.1, the greater the gradient express the more image edge details and information which are contained, and the image definition is higher. According to table 5.1, the method of this chapter can be better than traditional methods to enhance edge details and texture characteristics of the fog-degraded image, improve the image definition.

6. VESSEL SEGMENTATION IN X-RAY IMAGE

In recent decades, medical imaging techniques such as X-ray angiography and computed tomography angiography (CTA) have aided the diagnosis of atherosclerosis to the highest degree. Angiography or arteriography is a medical imaging technique used to visualize the inside, or lumen, of blood vessels and organs of the body, with particular interest in the arteries, veins and the heart chambers. This is traditionally done by injecting a radio-opaque contrast agent into the blood vessel and imaging using X-ray based techniques such as fluoroscopy. In this way, vessel analysis in medical images and videos is one of the most important research fields since it is appropriate in diagnostic and intervention planning purposes. For various visualization applications such as multi planar reformats or endovascular views, extraction of vessel centerline can be employed to generate particular visualization information. Also, for some of other applications including quantification, e.g. for determining the dimension of stents or stenosis grading, vessel segmentation can play an important role.

In this method, vessel segmentation in X-ray angiographic frame is realized using some experts which are in tandem. Firstly Hessian based vessel enhancement filter (HBVF) is applied to the angiographic frame to be segmented for enhancement of vessel structures. Afterward, angiographic frames in the sequence and their vesselness filtered versions are fused using 2-D wavelet transform to make an image which is used as a threshold for detecting the vessels. Finally, for detecting the vascular structures the fused image accompanying with a couple of thresholds is applied to the vesselness filtered frame to be segmented.

6.1 VESSELNESS FILTER

The main purpose of this filter is to extract vascular structures. To this aim, the eigen system of the Hessian matrix is analyzed by the filter to determine the curvature direction of image which is necessity for detection of vascular structures. Curvature direction in each point is the direction according to eigenvector of Hessian matrix in which the second order of image information is extremum.

6.1.1 Hessian Matrix

Hessian matrix or Hessian is a square matrix of second-order partial derivatives of a function. It describes the local curvature of a function of many variables. Eq() presents Hessian matrix which determines the second order information of 2D image.

$$I(x, y) \rightarrow H = \begin{bmatrix} \frac{\partial^2 I}{\partial x^2} & \frac{\partial^2 I}{\partial x \partial y} \\ \frac{\partial^2 I}{\partial x \partial y} & \frac{\partial^2 I}{\partial y^2} \end{bmatrix} \quad (19)$$

$$H = \begin{bmatrix} I_{xx} & I_{xy} \\ I_{yx} & I_{yy} \end{bmatrix} \quad (20)$$

Where H and I denote Hessian matrix and original image and I_{xx} , I_{yy} , I_{xy} and I_{yx} denote second derivative of image, respectively. Next, eigenvalues and eigenvector for Hessian matrix are computed. Based on eigenvalues of Hessian matrix, numerous vesselness filters are proposed out of which we use Frangi Vesselness Filter.

6.1.2 Frangi Vesselness Filter

In his seminal 1998 paper, Frangi introduced three measures to describe structure in images:

R_A : makes distinction between plate and line like structures

R_B : investigates deviation from a blob like structure

S : differentiates between vessels and background.

These measures are combined in a vesselness function as:

$$f(\lambda) = \begin{cases} 0 & \lambda_2 > 0 \\ e^{-\frac{R_B^2}{2\beta^2}} \cdot \left(1 - e^{-\frac{S^2}{2c^2}}\right) & otherwise \end{cases} \quad (21)$$

$$R_B = \frac{\lambda_1}{\lambda_2} \quad (22)$$

This ratio attains its maximum for a blob-like structure and is zero whenever $\lambda_1 \approx 0$, or λ_1 and λ_2 tend to vanish (notice that λ_1/λ_2 remains bounded even when the second eigenvalue is very small since its magnitude is always larger than the first). The parameters β , c adjust the influence of R_A , R_B and S .

To determine vesselness response, Hessian with Gaussian derivatives at multiple scales is computed and the highest response is considered as the output of the filter.

2D			3D		Orientation Pattern
λ_1	λ_2	λ_1	λ_2	λ_3	
N	N	N	N	N	Noisy, no preferred direction
		L	L	H-	Plate like structure(bright)
		L	L	H+	Plate like structure(dark)
L	H-	L	H-	H-	Tubular structure(bright)
L	H+	L	H+	H+	Tubular structure(dark)
H-	H-	H-	H-	H-	Blob-like structure(bright)
H+	H+	H+	H+	H+	Blob like structure(dark)

Table 6.1 Possible patterns in 2D and 3D, depending on the value of the eigenvalues λ_k (H=high, L=low, N=noisy, usually small, +/- indicate the sign of the eigenvalue). The eigenvalues are ordered: $|\lambda_1| \leq |\lambda_2| \leq |\lambda_3|$.

6.2 VESSEL SEGMENTATION

After applying the vesselness filter to the angiographic frame, the structures like vessels become more visible. However, in the background there are some particles such as ribs that take a great value due to applying the vesselness filter. As a result of applying the filter to such structures, the vessel segmentation algorithm results in error. As a remedy, in this approach we use information obtained from different angiographic frames to filter out the non vessel structures. The vessel pixels take low intensity levels in the angiographic frame while their intensity levels in the filtered image are higher than the background. Consequently, for detecting the vessels a threshold can be applied to the vesselness filtered image.

For fusing two images, filtered image and negative of original image, after decomposition step, we use pixel based fusion rule in which the coefficient of the fused image is obtained by averaging the corresponding db1 wavelet coefficient in filtered image and negative of original image.

Adjusting the threshold parameter (TH) for detection of vessels is a critical task because applying a high threshold value can remove some of vessel structures while a low threshold value cannot filter out non-vessels. To cope with the problem of vessel segmentation, firstly a high level threshold is applied to the image to remove most of non-vessels from image. Subsequently, the remaining vessels are detected and their directions are obtained for

recovering the removed parts. Afterward, according to the obtained direction structure element for dilation operator is constructed (as a binary matrix) and it is employed to expand the remaining vessels as a recovering step. This yields some false positives in the detected vessels. To reduce the false positives in the yielded image, a low level threshold is applied on the vesselness filtered image. Finally product of two images is considered as the result of the approach.

6.3 ALGORITHM

1. Compute the Hessian Matrix of the X-Ray Angiographic image using Eq ().
2. Calculate the eigen values and eigen vectors of the Hessian Matrix.
3. Based on the absolute values of eigen values, apply Frangi Vesselness Filter to the image. Adjust the parameters β and c according to the image.
4. Take negative of the original image and apply 2D Discrete Wavelet Transform using db1 wavelet.
5. Apply 2D Discrete Wavelet Transform on the filtered image using db1 wavelet.
6. Fuse the two images obtained after decomposition using pixel based fusion rule in which the coefficient of the fused image is obtained by averaging the corresponding db1 wavelet coefficient in filtered image and negative of original image.
7. Take the Inverse Wavelet Transform of the fused image.
8. Apply a suitable high threshold to the obtained image to remove false detection of vessels. Then apply a low threshold.
9. Perform opening and closing operation on the two images respectively and add them.
10. Vessels are extracted successfully in the final image.

6.4 RESULT & DISCUSSION

MATLAB R2008.0 has been used for simulations and demonstration of the proposed idea. X-Ray Angiographic image of the retina is taken as the input image on which Frangi Filter is applied. After fusion and thresholding, vessels are successfully segmented from the input image.

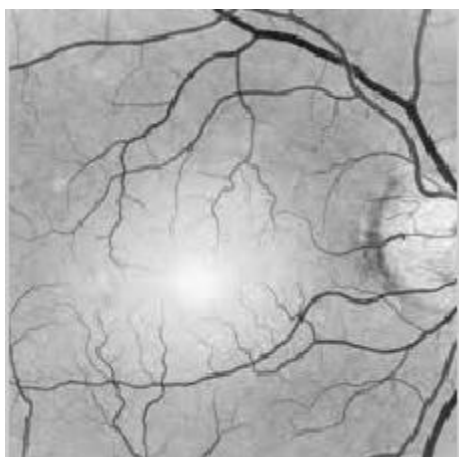


Fig 6.1 Original Angiographic Image

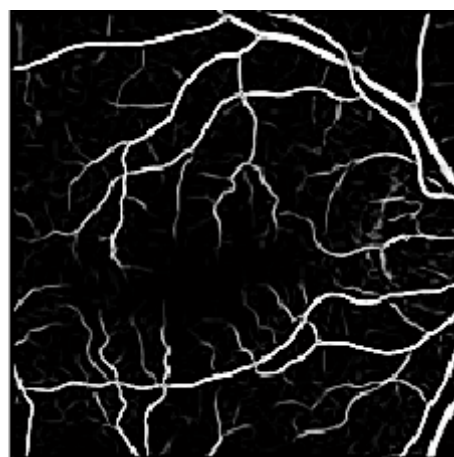


Fig 6.2 Vesselness Filtered Image



Fig. 6.3 Fused Image



Fig. 6.4 High Threshold Image



Fig. 6.5 Low Threshold Image



Fig. 6.6 Combined Final Image

7. TEXTURE FUSION OF CT/MRI IMAGES

A computed tomography (CT) scan is an imaging method that uses x-rays to create pictures of cross-sections of the body. Magnetic resonance imaging (MRI) is a medical imaging technique used to investigate the anatomy and function of the. MRI scanners use strong magnetic fields and radio waves to form images of the body. Because of a different imaging mechanism and high complexity of body tissues and structures, MRI and CT techniques provide non-overlay and complementary information. For instance, CT can clearly express human bone information, but it can not distinguish the soft tissue details; oppositely, MRI can clearly express soft tissue information, but it is not sensitive to bone tissue. Fusing CT and MRI images can get a complete picture which contains both clear bone tissue and soft tissue formation.

In this chapter, we present a wavelet-based texture fusion of CT/MRI images. Wavelet transform is employed to extract energy and regional information entropy of texture features from images. In the process of fusion, we adopt the fusion rule of energy maximum for the wavelet low-frequency coefficients; give the fusion rule according to the comparison of energy and regional information entropy contrast between CT/MRI images for the wavelet high frequency coefficients. Finally, obtain the fused medical image via inverse wavelet transform. We select two groups of CT/MRI images to simulate, and compare our simulation results with the most common wavelet transform fusion algorithm.

7.1 TEXTURE FEATURE EXTRACTION

The purpose of texture feature extraction is to get characteristic vector of every pixel which can be used to distinguish a different texture pattern. The results of two dimensional wavelet decomposition reflect frequency changes of different direction, also reflects the texture features of images. We select the energy and regional information entropy to express texture features of image.

1. Energy: When the image has more obvious texture features in a certain frequency bands or direction, the corresponding wavelet channel output has larger energy. The bigger energy of corresponding pixel is, the clearer texture feature is. The energy of image is described as below:

$$E = \frac{\sum_{i=1}^M \sum_{j=1}^N [f(i,j)]^2}{M \times N} \quad (23)$$

Where, $f(i, j)$ represent pixel gray value of point (i, j) . $M*N$ is the size of the image.

2. Regional Information Entropy: Entropy represents the average information of the image. The bigger entropy is, the richer details contained in image. It can also be measure criterion of image texture complexity. The entropy value is 0 when no texture is in the image. The entropy is maximized when full of texture is in the image. Regional Information Entropy is defined as:

$$H = - \sum_{i=1}^M \sum_{j=1}^N p_{ij} \log_2 p_{ij} \quad (24)$$

$$p_{ij} = \frac{f(i,j)}{\sum_{i=1}^M \sum_{j=1}^N f(i,j)} \quad (25)$$

Where H represents the regional information entropy, p_{ij} is the gray value probability of point (i, j) in the regional image, $f(i, j)$ is the gray value of point (i, j) in the regional image. The size of the region is $M*N$.

The procedure of texture feature extraction is:

- To implement two-dimension discrete wavelet decomposition (DWT) to each source image on the level of N , and obtain $3N+1$ sub-image.
- To calculate energy of all sub-images and regional information entropy of high frequency sub-images on each level.
- To express the image texture feature as $\{E_{LL} E_{LH} E_{HL} E_{HH} H_{LH} H_{HL} H_{HH}\}$.

7.2 WAVELET BASED TEXTURE FUSION

Image texture feature mainly displays in details, wavelet high-frequency coefficients just reflect the image details. So the feature extracted from the high frequency detail coefficients can give expression to the main feature of image texture.

7.2.1 Fusion of High Frequency Coefficients

The fusion of high-frequency coefficients is the key of image fusion. High-frequency coefficients contain image detail information of edge and texture, the processing of high frequency coefficients directly impact on the clearness and edge distortion of image.

1. Calculate energy and entropy of high frequency components.
2. Calculate Regional information entropy contrast according to the given formula:

$$KH_A^l(i, j) = \frac{H_A^l(i, j)}{H_A^H(i, j) + H_A^V(i, j) + H_A^D(i, j)} \quad (26)$$

$$KH_B^l(i, j) = \frac{H_B^l(i, j)}{H_B^H(i, j) + H_B^V(i, j) + H_B^D(i, j)} \quad (27)$$

Where $KH_A(i, j)$ and $KH_B(i, j)$ are regional information entropy contrast of image A and B, and they represent the proportion of high frequency components in one direction l(horizontal, vertical or diagonal) in the high frequency.

3. Select appropriate fusion rule: If the energy and regional information entropy contrast of image A are greater than or equal to image B at the same time, we select wavelet coefficients of image A as high-frequency coefficients. If the energy and regional information entropy contrast of image A are less than image B, we select wavelet coefficients of image B as high-frequency coefficients. If the energy and regional information entropy contrast of image A are not greater than or less than image B at the same time, high frequency components are described as follows:

$$f_H(i, j) = \frac{(\alpha f_A(i, j) + \beta f_B(i, j)) + (\mu f_A(i, j) + \nu f_B(i, j))}{2} \quad (28)$$

$$\alpha = \frac{E_A^l}{E_A^l + E_B^l} \quad (29)$$

$$\beta = \frac{E_B^l}{E_B^l + E_A^l} \quad (30)$$

$$\mu = \frac{KH_A^l}{KH_A^l + KH_B^l} \quad (31)$$

$$\nu = \frac{KH_B^l}{KH_A^l + KH_B^l} \quad (32)$$

$f_A(i, j)$, $f_B(i, j)$ respectively represent high frequency coefficients pixel value of fused image, image A and B at point (i, j). E_A and E_B respectively represent energy of high-frequency coefficients. l represents the horizontal, vertical and diagonal directions of image.

7.2.2 Fusion of Low Frequency Coefficients

Low-frequency coefficients contain most energy of image and represent the approximate image information. So we adopt energy maximum fusion rule for the low-frequency coefficients.

$$f_L(i, j) = \begin{cases} f'_A(i, j), & E'_A > E'_B \\ f'_B(i, j), & \text{else} \end{cases} \quad (33)$$

$f'_L(i, j)$, $f'_A(i, j)$ and $f'_B(i, j)$ respectively represent low frequency coefficients pixel value of fused image, image A and B at point (i, j). E'_A , E'_B respectively represent energy of low-frequency coefficients.

7.3 ALGORITHM

1. Take two images, one CT image and one MRI image.
2. Compute 2D Discrete Wavelet Transform of the two images and obtain the approximate and detailed coefficients.
3. Divide the coefficient matrices into 4X4 blocks and calculate energy of approximate and detailed coefficients and entropy of only detailed coefficients.
4. Calculate regional information entropy contrast of the detailed coefficients.
5. For high frequency coefficients (detailed coefficients) apply fusion rule as given above.
6. For low frequency coefficients (approximate coefficients) apply fusion rule as given above.
7. Obtain the final fused image by taking the inverse discrete wavelet transform.

7.4 COMPARISON WITH OTHER METHOD

The most common wavelet transform fusion algorithm is the weighted averaging rule for the low-frequency coefficients, and the rule of absolute value maximum for the high frequency coefficients. As can be seen by the simulation results, the image is fuzzy with this method whereas the fused image is clear with the presented method: both bone tissue and soft tissue can be distinctly reflected.

7.5 RESULT & DISCUSSION

Two sets of images are taken as input images. The first set has MRI and CT images of brain which are successfully fused together using the proposed fusion rule. The second set has MRI and CT images of the abdomen which are also successfully fused together using the proposed fusion rule.

SET 1: MRI and CT images of brain are used as input images

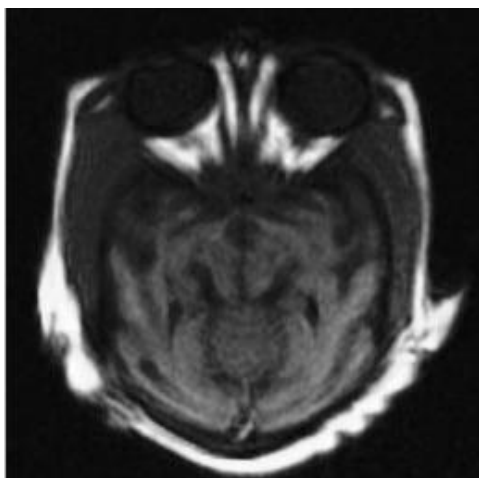


Fig. 7.1 MRI of brain

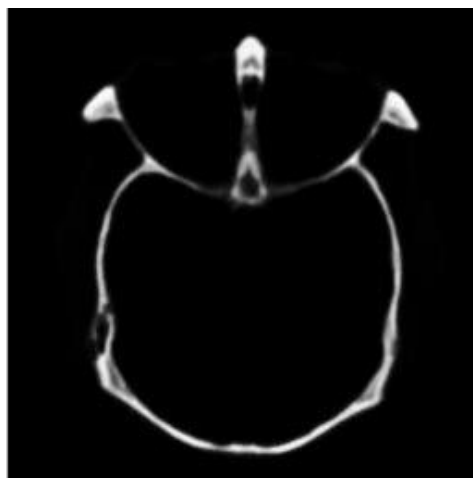


Fig. 7.2 CT scan of brain

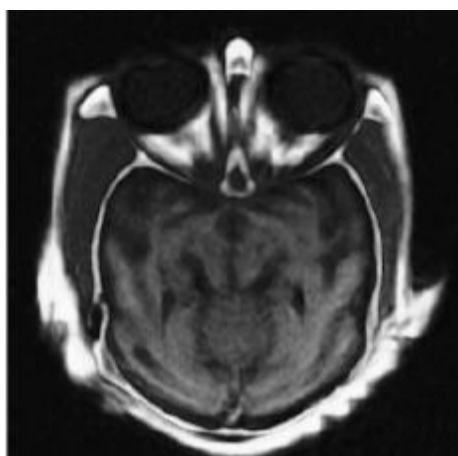


Fig. 7.3 Fused image by the proposed method

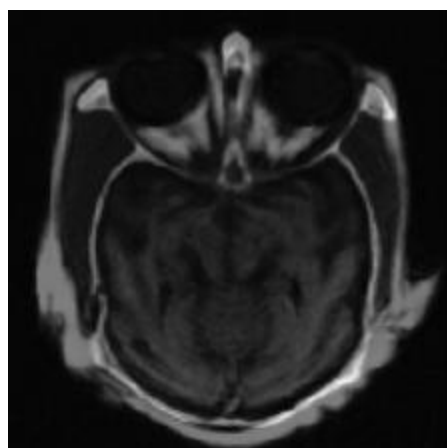


Fig. 7.4 Fused image by other method

SET 2: MRI and CT images of abdomen are used as input

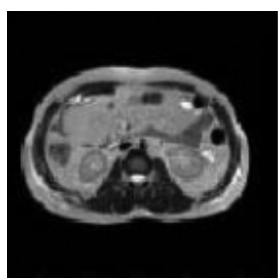


Fig. 7.5 MRI of abdomen

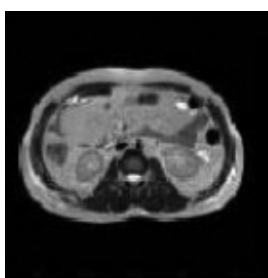


Fig. 7.6 CT of abdomen

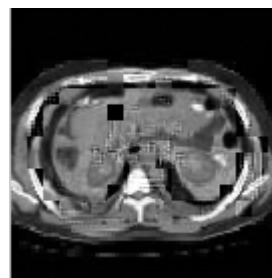


Fig. 7.7 Fused image

8. HIGH CAPACITY STEGANOGRAPHY

Steganography is the art and science of writing hidden messages in such a way that no one apart from the intended recipient knows of the existence of the message; this is in contrast to cryptography, where the existence of the message itself is not disguised, but the content is obscured. The advantage of steganography over cryptography alone is that messages do not attract attention to themselves, to messengers, or to recipients.

Steganographic messages are often first encrypted by some traditional means, and then a cover text is modified in some way to contain the encrypted message, resulting in stego text. For example, the letter size, spacing, typeface, or other characteristics of a cover text can be manipulated to carry the hidden message; only the recipient (who must know the technique used) can recover the message and then decrypt it. Steganography uses in electronic communication include steganographic coding inside of a transport layer, such as an MP3 file, or a protocol, such as UDP.

The objective for making steganographic encoding difficult to detect is to ensure that the changes to the carrier (the original signal) due to the injected payload (the signal to covertly embed) are visually (and ideally, statistically) negligible; that is to say, the changes are indistinguishable from the noise floor of the carrier.

8.1 AN OVERVIEW OF INTERNET SECURITY

Since the rise of the Internet one of the most important factors of information technology and communication has been the security of information. Everyday tons of data are transferred through the Internet through e-mail, file sharing sites, social networking sites etc to name a few. As the number of Internet users rises, the concept of Internet security has also gain importance. The fiercely competitive nature of the computer industry forces web services to the market at a breakneck pace, leaving little or no time for audit of system security, while the tight labour market causes Internet project development to be staffed with less experienced personnel, who may have no training in security. This combination of market pressure, low unemployment and rapid growth creates an environment rich in machines to exploited, and malicious users to exploit those machines.

8.2 STEGANOGRAPHY TECHNIQUES

Over the past few years, numerous steganography techniques that embed hidden messages in multimedia objects have been proposed. There have been many techniques for hiding information or messages in images in such a manner that alteration made to the image is perceptually indiscernible. Commonly approaches are including LSB, Masking and filtering and Transform techniques.

8.2.1 Least significant bit (LSB) insertion

It is a simple approach to embedding information in image file. The simplest steganography techniques embed the bits of the message directly into least significant bit plane of the cover-image in a deterministic sequence. Modulating the least significant bit does not result in human perceptible difference because the amplitude of the change is small. In this technique, the embedding capacity can be increased by using two or more least significant bits. At the same time, not only the risk of making the embedded message statistically detectable increase but also the image fidelity degrades. Hence a variable size LSB embedding schema is presented, in which the number of LSBs used for message embedding/extracting depends on the local characteristics of the pixel. The advantage of LSB-based method is easy to implement and high message pay-load.

Although LSB hides the message in such way that the humans do not perceive it, it is still possible for the opponent to retrieve the message due to the simplicity of the technique. Therefore, malicious people can easily try to extract the message from the beginning of the image if they are suspicious that there exists secret information that was embedded in the image.

Masking and filtering techniques, usually restricted to 24 bits and gray scale image, hide information by marking an image, in a manner similar to paper watermarks. The technique perform analysis of the image, thus embed the information in significant areas so that the hidden message is more integral to cover image than just hiding it in the noise level.

8.2.2 Transform techniques

Transform techniques embed the message by modulating coefficient in a transform domain, such as the Discrete Fourier Transform, or Wavelet Transform. These methods hide messages in significant areas of the cover image, which make them more robust to attack. Transformations can be applied over the entire image, to block throughout the image, or other variant.

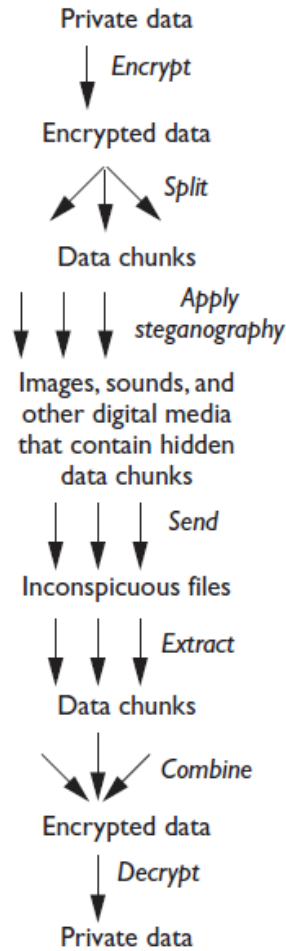


Figure 8.1 Process flow of secretly transmitting data. Using steganography, private data remains undetectable until it reaches its intended audience.

8.3 HIGH CAPACITY AND SECURITY STEGANOGRAPHY

In the Steganography systems, our main aim is to provide more capacity, security and maintain the quality of the cover image. The capacity requirements are usually met by techniques in spatial domain, whereas transform domain provides high robustness against attacks and eavesdropping. As a result, most of the non-fragile watermarking algorithms use transforms domain techniques because of their need for robustness, while spatial domain hiding methods are more attractive in steganography schemes due to the capacity concerns.

Our project aims at utilizing the Wavelet transform of the Cover image and the Payload colour data. The two-dimensional Wavelet transform decomposes the colour images into four bands, the LL, HL, LH and HH band which represents the low pass approximation, vertical, horizontal, and diagonal features of the colour image, respectively. These three bands convey the details of the image. We do the same decomposition on the LL quadrant.

Normally, after embedding the data into the image, the image may lose its resolution. In the proposed approach, Image Steganography has been designed to embed information in images while maintaining/enhancing the image quality.

The common modern technique of steganography exploits the property of the media itself to convey a message.

The following media are the candidates for digitally embedding message

- Plaintext
- Still imagery
- Audio and Video
- IP datagram

8.4 STILL IMAGERY STEGANOGRAPHY

The most widely used technique today is hiding of secret messages into a digital image. This steganography technique exploits the weakness of the human visual system (HVS). HVS cannot detect the variation in luminance of colour vectors at higher frequency side of the visual spectrum. A picture can be represented by a collection of colour pixels.

The idea behind the proposed algorithm is wavelet based addition. It involves adding of the wavelet decomposition of the normalized version of all the three (RGB) components (Red, Blue, and Green) of the cover image and the payload into a single fused result and then combining them to form the original colour image.

8.5 DATA HIDING REQUIREMENTS

8.5.1 Invisibility

The stego or the modified image should not appear to have gone under manipulation. This means that when one sees the image he must feel the image to be just another image in transmission. This lets the image not being suspected in any reason. This characteristic of the stego or the modified image is desired to be in the highest grade or degree.

8.5.2 Hiding capacity

The number of secret bits that can be hidden into the host image should be as large as possible. It is a desired thing that the size of the secret data file must be smaller than the host image or the original image file

8.5.3 Data security

The embedded secrets must be secure. This simply means that the secret message cannot be extracted by the illegal user. When one sees the image he must feel the image to be just another image in transmission. Also the method which is used must be secret enough to accomplish the desired task. In this project we have used the LSB substitution method.

8.6 ALGORITHM

The embedding and extraction algorithms have been explained below

8.6.1 Embedding

1. Take a payload image of size greater (double in this case) than cover image.
Cover image: 512 by 512 pixels.
Payload image: 1024 by 1024 pixels.
2. Separate Red, Blue and Green components of both the cover and Payload colour images.
3. Pre-processing is done on both the group of image components.
4. Compute 2D DWT of RGB components of cover and payload image using HAAR Wavelet.
5. Compute 2nd level DWT for the payload image.
6. Wavelet fusion of DWT coefficients of consequent components of 1st level DWT of Cover image and 2nd level DWT of Payload Image.
$$M(x, y) = C(x, y) + \alpha P(x, y) \quad (34)$$
7. Compute IDWT of all the Fused Red, Blue and Green components.
8. Combine the Red, Blue and Green components thus obtained to form the fused colour image.

8.6.2 Extraction

1. Separate Red, Blue and Green components of both the cover and Stego colour images.
2. Pre-processing is done on both the group of image components.

3. Compute 2D DWT of RGB components of cover and Stego image using HAAR Wavelet.
4. Subtract the DWT coefficients of the consequent components (RGB) of the Stego and the Cover Image.
5. Compute IDWT of all the subtracted Red, Blue and Green components.
6. Combine the Red, Blue and Green components thus obtained to form the fused colour image.

8.7 ANALYSIS

For finding out the quality of the Stego image generated we employ certain Image quality parameters. The good visual quality of stego images is the most important property of steganography system because it is hard to detect by detectors.

8.7.1 Signal to noise ratio (SNR)

This value gives the quality of reconstructed signal. The value should be on the higher side. It is given by

$$SNR = 10 \log_{10} \frac{\sigma_x^2}{\sigma_s^2} \quad (35)$$

8.7.2 Peak signal to noise ratio (SNR)

We use Peak Signal to Noise Ratio (PSNR) to measure the distortion between an original cover image and stego image.

The PSNR and MSE of cover image verses stego image are given by

$$PSNR = 10 \frac{\log_{10}(255)^2}{MSE} \text{ dB} \quad (36)$$

$$MSE = \frac{1}{MN} \sum_{j=1}^M \sum_{k=1}^N (x_{j,k} - x'_{j,k}) \quad (37)$$

MSE is the mean square error representing the difference between the original cover image sized $N \times N$ and the stego image sized $N \times N$, and the $x(j,k)$ and $x'(j,k)$ are pixel located at the j th row the k th column of images x and x' , respectively. A large PSNR value means that the stego image is most similar to original image and vice versa. It is hard for the human eyes to distinguish between original cover image and stego image when the PSNR ratio is larger than 30dB.

8.8 RESULT AND DISCUSSION

In this case we are usually choosing two images, the cover image of size (512×512) and the payload image of size (1024×1024) which indicates that size of payload image is greater than cover image and hiding such a large image (payload image) into a smaller image (cover image) without degrading the quality of the cover image indicates the high capacity of the algorithm and also the quality trade off.

MATLAB R2008.0 has been used for simulations and demonstration of the proposed idea. To evaluate the quality of the stego image, mean square error, SNR and PSNR between the stego image and the original image have been calculated and satisfactory results were obtained indicating the acceptable quality of the stego image generated by the algorithm.

After that it was possible to successfully extract the Payload image from the Stego image as shown in the figure.

The results below have been computed for 4 different values of alpha (α). SNR, MSE and PSNR are mentioned for each case.

1). $\alpha = 0.007$



Fig. 8.2 Cover image, Payload image, Stego image and Extracted image for $\alpha = 0.007$

SNR

- $\text{snr_red} = 17.0597$
- $\text{snr_green} = 19.9325$
- $\text{snr_blue} = 13.5006$

$\text{MSE} = 3.0863\text{e}+005$

$\text{PSNR} = -6.7296$

2). $\alpha = 0.02$



cover image



payload image



stego image, $\alpha = 0.02$



extracted image

Fig. 8.3 Cover image, Payload image, Stego image and Extracted image for $\alpha = 0.02$

SNR

- $\text{snr_red} = 17.1942$
- $\text{snr_green} = 19.9605$
- $\text{snr_blue} = 13.5703$

$\text{MSE} = 2.5194\text{e}+006$

$\text{PSNR} = -15.8483$

3). $\alpha = 0.07$



cover image



payload image



stego image, alpha = .07



extracted image

Fig. 8.4 Cover image, Payload image, Stego image and Extracted image for $\alpha = 0.07$

SNR

- $\text{snr_red} = 17.6977$
- $\text{snr_green} = 20.0693$
- $\text{snr_blue} = 13.8419$

MSE = 3.0863×10^{-7}

PSNR = -26.7296

4). $\alpha = 0.3$



cover image



payload image

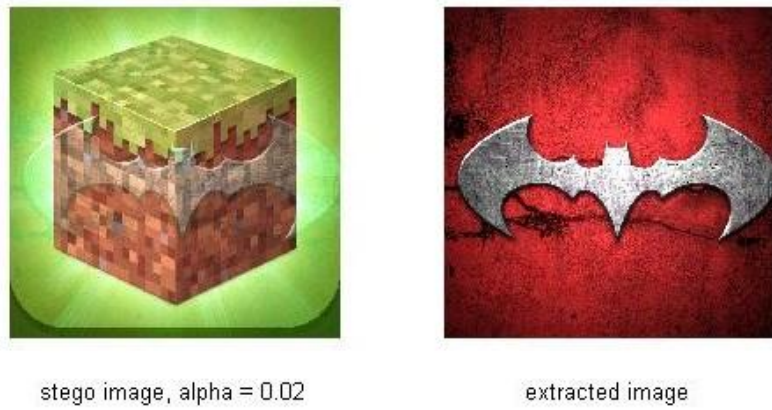


Fig. 8.5 Cover image, Payload image, Stego image and Extracted image for $\alpha = 0.07$

SNR

- snr_red = 19.7570
- snr_green = 20.5934
- snr_blue = 15.1235

MSE = 5.6688e+008

PSNR = -39.3701

(α)	SNR (red component)	SNR (green component)	SNR (blue-component)	PSNR
0.007	17.0597	19.9325	13.5006	6.7296
0.03	17.1942	19.9605	13.5703	15.8483
0.07	17.6977	20.0693	13.8419	26.7296
0.3	19.7570	20.5934	15.1235	39.3701

Table 8.1 Performance Analysis for different values of α

CONCLUSION

Various fusion algorithms were applied to images for texture classification, image enhancement, medical images, and data hiding in images. Images were first transformed to wavelet domain and then fusion algorithms were applied. Performance parameters related to the underlying problems were evaluated with interpretation and validation of results.

Wavelet analysis is a powerful tool since it segregates the regions according to information capacity. When a signal is transformed to wavelet domain, most of the information is packed in the low frequency components and hence they become the principal components.

Fusion algorithms when combined with wavelet domain provide better results for the above mentioned applications as compared to the spatial domain.

REFERENCES

1. G. S. Narasimhan and K. S. Nayar, "Contrast restoration of weather degraded images," IEEE Transactions on Pattern Analysis and Machine Intelligence, vol. 25, 2003, pp.713-724.
2. Yishu Zhai and Xiaoming Liu, "An improved fog-degraded image clearness algorithm," Journal of Dalian Maritime University, No.3, vol. 33, 2007, pp.55-57.
3. Heng Zhang ; Qing Ye, "Fog-Degraded Image Clearness Based On Wavelet Fusion", IEEE International Conference on Intelligent System Design and Engineering Application (ISDEA), Vol. 1, 2010, pp. 759 – 761.
4. Lizhi Cheng and Hongxia Wang, "Wavelet theory and applications," Science Press, Beijing, Sep 2004.
5. Bing Yin and Mei Yu, "Image enhancement using wavelet based contourlet transform," Computer Engineering and Design, No.12, vol. 29, 2008, pp.3142-3144.
6. <http://blogs.mathworks.com/steve/2013/07/10/homomorphic-filtering/>
7. http://cache.freescale.com/files/dsp/doc/app_note/AN4318.pdf
8. Artz, D. ; Los Alamos Nat. Lab., NM, USA, "Digital steganography: hiding data within data", Internet Computing, IEEE (Volume:5 , Issue: 3), 07 August 2002, pp. 75-80
9. Sidhik, S. ,Sudheer, S.K. ; Mahadhevan Pillisai, V.P., "Modified high capacity steganography for color images using wavelet fusion", Fiber Optics in Access Network (FOAN), 2013 4th International Workshop, 11-12 Sept. 2013, pp. 40-43
10. S. E. El-Khamy, M. Khedr, A. AlKabbany, "A data hiding technique"25th NRCS, March 2008L
11. Prabakaran, G. Bhavani, R., "A modified secure digital image steganography based on Discrete Wavelet Transform", Computing, Electronics and Electrical Technologies (ICCEET), 2012 International Conference, 21-22 March 2012, pp. 1096-1100
12. Paul Hill, Nishan Canagarajah and Dave Bull, "Image Fusion using Complex Wavelet", Dept. of Electrical and Electronic Engineering, The University of Bristol.
13. Marius Staring¹, Changyan Xiao, Denis P. Shamonin, and Berend C. Stoel "Pulmonary Vessel Segmentation using Vessel Enhancement Filters", College of Electrical and Information Engineering, Hunan University, China
14. Alejandro F. Frangi, Wiro J. Niessen, Koen L. Vincken, Max A. Viergever, "Multiscale vessel enhancement filtering", In Medical Image Computing and computer-assisted Intervention-MICCAI'98, W.M. Wells, A. Colchester and S.L Delp(Eds.), Lecture Notes in Computer Science, vol. 1496-Springer Verlag, Berlin, Germany,pp. 130-137

15. M.J.Rastegar Fatemi, Seyed Mostafa Mirhassani and Bardia Yousefi “Vessel Segmentation in X-ray Angiographic Images Using Hessian Based Vesselness Filter and Wavelet Based Image Fusion” Information Technology and Applications in Biomedicine (ITAB), 2010 10th IEEE International Conference, 3-5 Nov. 2010
16. Jionghua Teng, Xue Wang, Jingzhou Zhang, Suhuan Wang, “Wavelet-based Texture Fusion of CT/MRI Images”, 2010 3rd International Congress on Image and Signal Processing, 16-18 Oct. 2010, pp. 2709 - 2713
17. Shih-Gu-Huang, “Wavelet for Image Fusion”, Graduate Institute of Communication Engineering & Department of Electrical Engineering, National Taiwan University.
18. M. Sifuzzaman, M.R. Islam and M.Z. Ali, “Application of Wavelet Transform and its Advantages Compared to Fourier Transform”, Journal of Physical Sciences, Vol. 13, 2009, 121-13.
19. Shaikhji Zaid M, Jagadish Jadhav R,P J Deore " An Efficient Wavelet based Approach for Texture Classification with Feature Analysis" 2013 3rd IEEE International Advance Computing Conference (IACC)
20. <http://www.nada.kth.se/cvap/databases/kth-tips/download.html>"
21. http://soest.hawaii.edu/sjara/roughness_references/sidescan/Haralick_et_all_73_Textural%20Features%20for%20Image%20Classification.pdf
22. <http://www.mathworks.in/help>
23. <http://wwwghcc.msfc.nasa.gov/land/ncrst/infoextract.html>